

Portland State University

PDXScholar

Dissertations and Theses

Dissertations and Theses

1992

The Tensile Strength of Liquid Nitrogen

Jian Huang

Portland State University

Follow this and additional works at: https://pdxscholar.library.pdx.edu/open_access_etds

Let us know how access to this document benefits you.

Recommended Citation

Huang, Jian, "The Tensile Strength of Liquid Nitrogen" (1992). *Dissertations and Theses*. Paper 1134.
<https://doi.org/10.15760/etd.1133>

This Dissertation is brought to you for free and open access. It has been accepted for inclusion in Dissertations and Theses by an authorized administrator of PDXScholar. Please contact us if we can make this document more accessible: pdxscholar@pdx.edu.

THE TENSILE STRENGTH OF LIQUID NITROGEN

by

JIAN HUANG

A dissertation submitted in partial fulfillment of the
requirements for the degree of

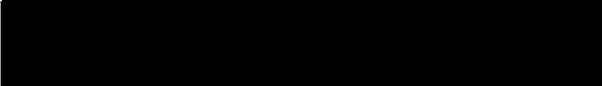
DOCTOR OF PHILOSOPHY
IN
ENVIRONMENTAL SCIENCES and RESOURCES:
PHYSICS

Portland State University
1992

TO THE OFFICE OF GRADUATE STUDIES:

The members of the Committee approve the dissertation of
Jian Huang presented May 7, 1992.


Erik Bodegom, Chair


Jack S. Semura



Laird C. Brodie



Stanley S. Hillman


Carole R. Gatz


Robert O'Brien

APPROVED:


John/G. Rueter Jr., Director, Environmental Sciences and
Resources Program


C. William Savery, Interim Vice Provost for Graduate
Study and Research

AN ABSTRACT OF THE DISSERTATION OF Jian Huang for the Doctor
of Philosophy in Environmental Science and Resources: Physics
Presented May 7, 1992.


Title: The Tensile Strength of Liquid Nitrogen.

APPROVED BY THE MEMBERS OF THE DISSERTATION COMMITTEE:

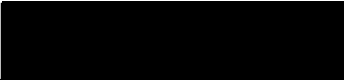

Erik Bodegom, Chair


Jack S. Semura


Laird C. Brodie


Stanley S. Hillman


Carole R. Gatz


Robert J. O'Brien

The tensile strength or the negative pressure required to induce cavitation in a pure liquid has been a puzzling subject. On one hand, the classical nucleation theory has met great success in predicting the nucleation rates of superheated liquids. On the other hand, most of reported

experimental values of the tensile strength for different liquids are far below the prediction from the classical nucleation theory. In this study, homogeneous nucleation in liquid nitrogen and its tensile strength have been investigated.

In order to carry out the measurement of the tensile strength of liquid nitrogen, different approaches for determining the pressure amplitude were studied carefully. It is shown that Raman-Nath theory, as modified by the introduction of an effective interaction length, can be used to determine the pressure amplitude in the focal plane of a focusing ultrasonic transducer. The results obtained from different diffraction orders are consistent and in good agreement with other approaches including Debye's theory and solving the KZK (Khokhlov-Zabolotskaya-Kuznetsov) equation. The results from experiments in water demonstrated that as long as the nonlinearity is not too large, the experimentally determined pressure follows closely the calculated results using either Debye's theory or the KZK equation. In addition, the light diffraction contains enough information to calculate the second-order harmonic in the sound wave. In principle, it is possible that the contribution to the acoustic wave of the higher than the second-order harmonic can be obtained.

The measurement of the tensile strength was carried out in a high pressure stainless steel dewar. A High intensity ultrasonic wave was focused into a small volume of liquid

nitrogen in a short time period. A probe laser beam passes through the focal region of a concave spherical transducer with small aperture angle and the transmitted light is detected with a photodiode. When the voltage on the transducer reaches a critical point, nucleation in the focal region occurs and a characteristic signal associated with the nucleation was obtained. At this moment, the pressure amplitude at the focus is calculated based on the acoustic power radiated into the liquid. In the experiment, the electrical signal on the transducer is gated at its resonance frequency with gate widths of 20 μ s to 0.2 ms and temperature range from 77 K to near 100 K. The calculated pressure amplitude is in agreement with the prediction of classical nucleation theory for the nucleation rates from 10^6 to 10^{11} (bubbles/cm³ sec).

This work enhances our understanding of the nucleation process in liquids. It provides the direct experimental support that the validity of the classical nucleation theory can be extended to the region of the negative pressure up to -90 atm. This is only the second cryogenic liquid to reach the tensile strength predicted from the classical nucleation theory.

ACKNOWLEDGEMENTS

I would like to express my sincere appreciation to the individuals who have offered friendship and assistance throughout my study here at Portland State. They have made this project possible. It has been an enjoyable experience to work with and learn from my advisor, Dr. Erik Bodegom. I am grateful to Dr. Bodegom not only for his generous and expert guidance throughout this work but also for his constant care and patience, untiring encouragement and support during the course of this project. I would like to thank the members of my advisory committee: Dr. Laird Brodie, Dr. Jack Semura, Dr. Stanley Hillman from Biology, Dr. Carole Gatz, and Dr. O'Brien for their advice, suggestions and precious time which they committed in addition to their research endeavors and heavy academic duties. I would also like to thank Dr. Joel Nissen whose work on liquid helium has laid the ground for this research, Eric Roth, my co-worker in this lab, whose technical assistance and friendship helped me a great deal. My thanks also to Margie Fyfield who helped me to correct the grammar and made numerous suggestions to this thesis. I would also like to thank Rudi Zupan who built the high pressure dewar and offered a lot of technical assistance, and Brian McLaughlin of the Science Support Shop. Finally, I would like to thank my family in China, my chinese friends here, and my American

family, the Kents, Boths, and Lelands. Above all, I thank my wife Hui for her unconditional support and encouragement. To my wife and my parents, this dissertation is dedicated.

TABLE OF CONTENTS

	PAGE
ACKNOWLEDGEMENTS.	iii
LIST OF TABLES.	vii
LIST OF FIGURES	viii
CHAPTER	
I OVERVIEW	1
Introduction	1
Cavitation and tensile strength of liquids	3
Background Observation of the Cavitation in a Liquid	
The Acoustic Cavitation in cryogenic liquids	9
Overview of the Dissertation	13
II HOMOGENEOUS NUCLEATION THEORIES AND TENSILE STRENGTH OF LIQUIDS.	15
Equation of State of Liquids	17
The Van Der Waals Theory of Liquids The Tensile Strength Calculated from the Virial Series	
Kinetic Theories of Homogeneous Nucleation	30
The Modification of Classical Nucleation Theory	45
III DETERMINATION OF PRESSURE IN A LIQUID	48
Determination of pressure amplitude by the light diffraction method.	50

	Revised Raman-Nath Theory Calculation of Pressure at the Focus from Debye's Theory The Pressure Distribution Calculated from the KZK Equation	
	Calculation of Pressure Amplitude in Water with Different Approaches	63
IV	MEASUREMENT OF THE TENSILE STRENGTH OF LIQUID NITROGEN	74
	The Design of the High Pressure Dewar . . .	75
	Experimental Setup and Measurement of the Parameters of the Transducer.	78
	Measurement	81
	Experimental Procedures	
	Measurement of the Tensile Strength of Liquid Nitrogen Using Raman-Nath Light Diffraction Method	
V	CONCLUSION	101
	REFERENCES	104
	APPENDIX	
A	CALCULATION OF THE SURFACE PRESSURE OF A TRANSDUCER	110
B	CORRECTION OF THE TEMPERATURE MEASUREMENT . .	120

LIST OF TABLES

TABLE		PAGE
I	Hard-sphere virial coefficients	28
II	Coefficients for liquid-vapor coexistence equation of nitrogen	38
III	Coefficients for saturated vapor pressure equation	40
IV	Coefficients for liquid density equation . .	40

LIST OF FIGURES

FIGURE		PAGE
1.	Andrews isotherms of liquid nitrogen for T _c , 110, 95, 85, 77, 67 K	20
2.	The tensile strength of liquid nitrogen predicted from the van der Waals equation as a function of the temperatures.	22
3.	P-V curve for T=110 K	23
4.	The saturated vapor and liquid densities of nitrogen vs. temperature	39
5.	The pressure in liquid nitrogen vs. temperatures for different nucleation rates	42
6.	Poynting correction vs. temperatures	44
7.	The diffraction light intensities of 0, 1st, -1st orders for different values of a ₂ =0, 0.01, 0.05, 0.1	54
8.	Measured light intensities relative to the intensity of the undiffracted beam for the zeroth, positive, and negative first diffraction orders vs. the applied voltage	65
9.	Pressure at the focal point vs. the surface pressure on the transducer calculated from zeroth-order diffraction, and comparison with the results from Debye's theory and the KZK equation	67
10.	Pressure at the focal point vs. the surface pressure on the transducer calculated from the diffraction order of +1, and comparison with the results from Debye's theory and the KZK equation	68
11.	Pressure at the focal point vs. the surface pressure on the transducer calculated from the diffraction order of -1, and	

	comparison with the results from Debye's theory and the KZK equation	69
12.	The axial pressure distributions calculated from the KZK equation with values of 0, 0.025, 0.1, 0.2 for the nonlinearity parameter B	71
13.	The transverse pressure distributions in the focal plane calculated from the KZK equation with values of 0, 0.025, 0.1, 0.2 for the nonlinearity parameter B. . .	72
14.	The stainless steel dewar built for measurement of the tensile strength of liquid nitrogen	77
15.	The diagram of the experimental setup for measuring the tensile strength of liquid nitrogen	79
16.	Schematic diagram of the light diffraction by a focused ultrasonic wave	80
17.	Schematic diagram of the electrical pulse applied to the transducer of 1 MHz	83
18.	Transmitted light intensity for different voltages on the transducer of 2 MHz . . .	86
19.	Transmitted light intensity for 1 MHz transducer with small aperture angle on different time scales.	87
20.	Transmitted light intensities for 1 MHz hemispherical transducer	88
21.	The electrical signals at the hemispherical transducer of 1 MHz	91
22.	The experimentally obtained data in comparison with the theory of homogeneous nucleation for different transducers of 1 MHz and 2 MHz respectively	93
23.	The intensity of transmitted light without the presence of the ultrasonic field	97
24.	Optical signal in real time and frequency domain for sampling frequency of 10 kHz	99
25.	Optical signal in real time and frequency domain for sampling frequency of 200 kHz	100

26.	The equivalent circuit of a focusing transducer	112
27.	The gate circuit measuring the impedance of the transducer	115
28.	Measured ratio of V_{in}/V_{out} as a function of frequency when the transducer is in air at room temperature	116
29.	Measured ratio of V_{in}/V_{out} as a function of frequency for the transducer in the water	117
30.	Measured ratios of V_{out}/V_{in} as functions of frequency for the transducer of 1 MHz in air and liquid nitrogen	118
31.	Measured ratios of V_{out}/V_{in} as functions of frequency for the transducer of 2 MHz in air and in liquid nitrogen	119

CHAPTER I

OVERVIEW

INTRODUCTION

Liquid to gas phase transitions are one of the most common physical phenomena in nature. A characteristic parameter associated with this process is the tensile strength of the liquid. The concept of the tensile strength is generally associated with solids such as metals and semiconductors but not liquids. The tensile strength of a solid material refers to the upper limit of the stress in the material when it breaks. Under appropriate conditions, liquids can also sustain considerable tensions. If this tension is sufficient the liquid also "breaks". This "break" manifests itself as cavitation, the name given to the production of a number of very small cavities or bubbles in the liquid. The tensile strength of a pure liquid is usually defined as the difference between the vapor pressure and that of the liquid when homogeneous nucleation occurs. Unlike heterogeneous nucleation which is induced by the impurities including dissolved gases and solid particles, or interfaces in the liquid, homogeneous nucleation is induced by structural fluctuations caused by the external condition in the pure liquid. The overall objective of this work is to measure the

homogeneous nucleation limit or the tensile strength of liquid nitrogen. It is reached by using a strongly focused ultrasonic field which is probed by a laser beam. In order to understand the mechanism of the homogeneous nucleation process by stretching liquid nitrogen acoustically, one needs not only to examine how the acoustic cavitation develops in liquid nitrogen, investigate the possible ways to determine how much acoustic energy that we put into the liquid and the maximum pressure amplitude at the focus for a given surface pressure at the transducer, but also explore techniques to detect the onset of homogeneous nucleation in liquid nitrogen. The research on this subject is basically an extension of Nissen's work (1988, 1989) on liquid helium, to liquid nitrogen.

This thesis is organized as follows. In Chapter I, we started from defining the problem of this research and then will describe the brief background and current research of tensile strength of liquids. In Chapter II, we will examine the homogeneous nucleation theories and revisit the concept of the tensile strength in liquids. The light diffraction method to determine the pressure amplitude and other techniques including traditional Debye's theory and KZK (Khokhlov-Zabolotskaya-Kuznetsov) equation are investigated in the Chapter III. In Chapter IV, we will describe our measurement of the tensile strength of liquid nitrogen in detail, analyze our data and present our experimental results. In Chapter V, we will discuss our experimental results, compare with those

obtained from classical nucleation theory and draw our conclusions. The equivalent circuit model to determine the parameters of a concave spherical transducer will be discussed in the Appendix.

CAVITATION AND TENSILE STRENGTH OF LIQUIDS

Background

Cavitation and the tensile strength of liquids are topics of interest in a number of fields in pure and applied science. The cavitation properties of the liquid coolant play a large part in the design and safety of fast nuclear reactors. In engineering "cavitation damage" is related to the design and performance of ship propellers, lubricating films in bearings and all kinds of hydraulic machinery. When a cavitation bubble collapses near the surface of a solid in contact with the liquid it usually develops a "spike" of liquid, called a microjet, which is directed towards the surface. It appears that there are two mechanisms responsible for the damage produced by a bubble collapse. There is damage caused by the impact of the microjet on the surface, and there is the effect of the radiated shock wave hitting the surface. In botany, cavitation and the tensile strength of water are related to the ascent of sap. We know that columns of sap transport water from the roots of a tree to the uppermost leaves. We also know that the atmosphere will support a column of water only 10.4 M high. But many trees are far taller than this.

When water evaporates through the leaf pores, there is evidence of the development of negative pressure in the capillaries of the leaves. It is this negative pressure which causes the ascent of sap. In medicine, cavitation effects occur in decompression sickness. This is a problem facing people who have been exposed to a raised atmospheric pressure for a length of time, for example deep sea divers. As we know, the pressure increases by one bar with every 10 M of depth. The oxygen, nitrogen and helium gases breathed into a diver's lungs at a fairly large depth dissolve more easily since their pressure is greater. They therefore diffuse more readily into the tissues of the body. If a diver surfaces too quickly, that is a rapid decompression occurs, gas bubbles will appear in his tissues and blood. The formation of these bubbles gives rise to decompression sickness, the most common type being the "bends" which manifest itself as a pain in the joints. In physics, these matters are related to metastable phases of a liquid and its equation of state. More recently as people found that trapped gas bubbles in some liquids can emit light, cavitation in liquids has received more attention in both basic and applied research. A potential application for cavitating liquids is as a new light source.

Observation of the Cavitation in A Liquid

A necessary condition for cavitation to occur is that the pressure somewhere in a liquid should drop below zero and become a tension. There are many ways to achieve this

condition such as direct application of a force to a solid or liquid boundary, thermal contraction of a liquid filling a solid vessel, application to the liquid of sufficiently intense ultrasound so that the pressure drops below zero for part of each cycle, reflection of pressure pulses by the free surface of a liquid or by a yielding solid boundary, evaporation of a liquid through a semi-permeable membrane, etc. In all these situations, the 'apparent tensile strength', i.e. the maximum tension when cavitation occurs, varies widely according to the liquid condition and type of experiment carried out. One has to distinguish carefully between three kinds of situations as follows. (a) The static application of tension. (b) The 'once-only' dynamic application of tension such as by reflection at the free surface of a liquid of the pressure pulse produced by an explosion. (c) The periodic application of tension. This can occur through the application of ultrasound to a liquid.

The static application of tension. The pioneer work attempting to measure the tensile strength of liquids was done by Marcellin Berthelot in 19th century. He developed the Berthelot tube method to measure the tensile strength of water and estimated the maximum negative pressure for water was between -30 and -50 atmospheres. Since then, many modifications and improvements have been made but the measured tensile strength of water is well below the theoretical prediction. The measured highest tensile strength for water

using regular static application of tension was reported by Briggs (1950). His value was around 277 atm. Green et al. (1990) studied water trapped in quartz and other crystals and they estimated the tensile strength of water is larger than 1000 atm. This is the highest experimental value ever reported for the tensile strength of water.

Dynamic stressing of a liquid. A liquid can be subjected to tension under so called 'one time only' dynamic stressing. One way is that a compressional pulse is first produced in the liquid and later converted into a tension pulse by reflection at a suitable boundary. However, most of the reported tensile strengths measured in water are much lower than that of theoretical predictions. Carlson and Henry (1973) used the reflection principle to convert a pressure pulse into a tension pulse. This was achieved by arranging for the pressure pulse to be reflected not at the free surface of the liquid but at a suitable liquid-solid interface. From a series of experiments Carlson and Henry found the breaking tension of glycerol to be 600 bar (1 bar=0.9869 atm). There have been many other methods reported and D.H. Trevena (1987) discusses those experiments in some detail.

Acoustic cavitation. In order to avoid the undesirable effects of solid container surfaces, the tension must somehow be exerted in a region a large enough distance away from the surface of the container. One way to accomplish this is to focus high-intensity ultrasonic waves on some region within

the liquid, generating a large alternating stress in it. As an ultrasonic wave propagates past any position in the liquid, the liquid experiences a compression and a tension during the positive and negative half periods, respectively. So during any part of one acoustic cycle the absolute pressure in the liquid is equal to the hydrostatic pressure plus the instantaneous acoustic pressure. The pressure in the liquid alternates back and forth from larger than the hydrostatic pressure to a pressure less than the hydrostatic pressure. If the amplitude of the acoustic wave is large enough, cavitation would be expected to occur during the negative half of the cycle. Then during the next compressional half cycle the cavities collapse and regrow in the successive negative half cycle.

Acoustic cavitation is characterized by the interaction of a sound field with vapor phase nuclei of appropriate size present in the exposed liquid. The radial motion of the bubble, caused by a pulsed ultrasonic field results in two different types of cavitation processes. First, the bubble experiences comparatively mild oscillations, where bubble radii change by a factor of less than two. That is often defined as stable cavitation. As the acoustic amplitude increases, the oscillation amplitude becomes larger and then develops into violent collapse known as transient cavitation. The tensile strength of a liquid is the local negative pressure at the moment when the transient cavitation occurs.

The transition from the stable to transient cavitation depends on the initial size of nuclei and the peak pressure of applied sinusoidal acoustic pulse.

The tensile strength measured by ultrasonic waves is also called the acoustic cavitation threshold. Since the negative pressure has limited time duration and is followed by the positive part of the cycle, the cavity is short-lived. A shock wave is produced during the violent collapse of the cavity, accompanying its disappearance. The acoustic cavitation threshold can be larger than the tensile strength measured by static means; not only must the cavity be created during the brief period of tensile stress but also it must grow significantly while the pressure is negative. If it does not grow enough, it may collapse completely during the positive part of acoustic cycle before it gets big enough to be observed. Therefore a maximum acoustic stress larger than the stress required to create the cavity may be needed. In practice, however, because of the periodic nature of the acoustic cavitation, the cavitation threshold depends on the acoustic pulse width, and repetition rate. With high repetition rate or larger pulse width, the cavitation threshold is found lower.

In order to observe the acoustic cavitation in a liquid, there must be at least one bubble created in the region in which we are interested. This condition is obviously time and volume dependent. The longer time we wait or the larger

volume we observe, the more likely that there is a bubble. The mathematical form of this necessary condition of forming a bubble spontaneously can be obtained simply from the rate equation

$$J(P, T) * V * \tau \geq 1 \quad (1.1)$$

where $J(P, T)$ is the nucleation rate per unit volume and unit time ($\text{cm}^3 \text{ sec}^{-1}$). J is a function of local pressure and temperature. V is the liquid volume that is studied and if it is sufficiently small, the heterogeneous nucleation can possibly be excluded. τ is the time period during which the liquid is stretched by means of the ultrasonic wave. τ represents the average expectation time of a bubble forming spontaneously with a radius larger than the critical radius and is different from the time needed to observe a bubble in a particular position in the volume V .

THE ACOUSTIC CAVITATION IN CRYOGENIC LIQUIDS

Cavitation is one of the most characteristic phenomena of cryogenic liquids. In normal water, cavitation arises only at considerable pressure reductions or high temperatures, while in cryogenic liquids, cavitation develops easily even without slight pressure pulsations. The reason is not only the difference between the static pressure and the pressure of saturated vapors. Cryogenic liquids have smaller values of surface tension than water, which also results in much smaller values of cavitation strength. For example, the tensile

strength of liquid nitrogen can be 10 times smaller at atmospheric pressure than that of water. Another advantage of the cryogenic liquids is that the effect of dissolved gas cavitation nuclei is negligible. This greatly reduces the possibility of heterogeneous nucleation in the cryogenic liquids. However, to get rid of cavitation nuclei altogether is practically impossible. In inadequately clean cryogenic liquids, solid particles of frozen gases and dust can become cavitation nuclei. In addition, in cryogenic liquids there can be cavitation nuclei in the form of vapor bubbles resulting from local heat release caused by imperfections in the thermal insulation of cryogenic systems, which leads to heat transmitted into liquid and its local boiling. In any cryogenic liquid, vapor bubbles generated by high energy particles are also present because under real conditions the background of cosmic rays and particles cannot be got rid of. Due to penetration of ionizing charged particles, such as electrons, mesons, protons and others into the liquid, there is local heat release. In very pure cryogenic liquids cavitation nuclei in the form of vapor bubbles induced by local heterophase fluctuations can also appear.

Similar to any other usual liquids, the acoustic cavitations in the cryogenic liquids can be divided into two classes. "Stable" cavities are bubbles that oscillate nonlinearly around some equilibrium size. They exist for many cycles of the sound field, but may grow or shrink slowly by

diffusion of vapor processes. On the other hand, "transient" cavities exist for only part of one acoustic cycle, after which they collapse and disintegrate into smaller bubbles. Neppiras and Finch (1972) studied the acoustic cavitation in liquid helium and nitrogen at low acoustic frequency near the boiling points and distinguished four types of bubble activity in those liquids. (a) accelerated boiling, with an increased density and growth rate of vapor bubbles; (b) generation of bubble clouds at high intensities; (c) accumulation and subsequent breakup of free vapor on the surface of acoustic transducer; and (d) audible effects including an intense subharmonic signal which was present whenever bubbles were seen and white noise which accompanied the cloud formations.

Although the cryogenic liquids have the advantages over usual liquids to test the homogeneous nucleation theory and their tensile strengths are easier to measure, most tensile strengths reported so far are well below the theoretical predictions. For example, several groups (Beams, 1956, Misener et al., 1956, Finch et al., 1964, 1966, Jarman et al., 1966) measured tensile strength of liquid helium to be much smaller than 4 atm which is the minimum value predicted from the theory of the equation of liquid state (Beams, 1956). Moreover, the experimental results are very dependent upon the methods used and thus they are not consistent. Therefore, people have been trying to modify the existing theory in order to explain the measured tensile strengths. By assuming there

are preexisting vapor nuclei in the liquids, Akulichev (1986) compared their theoretical tensile strengths with those measured in liquid hydrogen, nitrogen (Hord et al., 1964) and found they are in relative good agreement. Up to date, the tensile strength of liquid helium predicted by the classical nucleation theory has been reached only by Nissen et al. (1988, 1989). They used a piezoelectric transducer in the form of a hemispherical shell to focus high-intensity ultrasound into a small volume of liquid helium. The transducer was gated at its resonant frequency of 566 kHz with gate widths of less than 1 msec in order to minimize the effects of transducer heating and acoustic streaming. They detected the onset of homogeneous nucleation and measured the strength of liquid helium by detected the presence of the nucleated bubbles by light scattering. Homogeneous nucleation occurred in the time period between when the ultrasonic wave arrived at the focal point and when rapid fluctuation were detected in the optical signal. In their discussion of the existing models, the equation of state takes the form of van der Waals equation. They used modified Raman-Nath theory to calculate the pressure amplitude at the focal region. His experimental results are in good agreement with the classical nucleation theory for a nucleation rate of approximately 10^{15} critical size bubbles/sec-cm³. This is only the third liquid for which the theoretical tensile strength has been reached and it confirms homogeneous nucleation theory over a range ten

times greater than any other experiment. However, Xiong and Maris later (1989, 1990) reexamined the theory of homogeneous nucleation and made an estimate of the equation of state for negative pressure in helium and calculated the tensile strength of liquid helium at $T=0$ K to be around -9 atm instead of $-\infty$ atm predicted by the classical nucleation theory. Since their revised model and classical nucleation theory disagreed most at temperatures below 1.5 K, they performed the tensile strength measurements between 0.8 K and 2.0 K by using the same method as Nissen and found that it is much lower than what Nissen measured. It is also lower than what is predicted by their theoretical model. Xiong and Maris explained this obvious discrepancy by the possible existence of vortices in helium in the presence of a sound field.

OVERVIEW OF THE DISSERTATION

Although the classical nucleation theory might fail when the temperature is close to 0 K because of either quantum tunneling or revision of the equation of state, it is reasonable to argue that the classical nucleation theory should stand when the temperature is not lower than 1.5 K. Furthermore, Sinha et al. (1987) used a transient superheating technique in liquid nitrogen to test the classical nucleation theory in the temperature range from 77 K to 125 K and found that their results are in good agreement with the prediction of classical nucleation theory. This dissertation is

focused on the tensile strength of liquid nitrogen and hopefully it will shed some light on the reasons for the discrepancies between Nissen's and Xiong and Maris' results. We intend to examine Nissen's method more closely and apply it to a different cryogenic liquid, liquid nitrogen. Liquid nitrogen is chosen as the liquid to study for several reasons. Liquid nitrogen is the least expensive, in virtually unlimited abundance and is one of the most widely used cryogenic liquids. The tensile strength of liquid nitrogen according to classical nucleation theory is in between that of liquid helium and water, and this pressure range is attainable by the instruments in our laboratory.

CHAPTER II

HOMOGENEOUS NUCLEATION THEORIES AND TENSILE STRENGTH OF LIQUIDS

Theoretical studies of metastable systems have long been of interest and they mainly follow two different routes. The first approach is as follows. One develops a kinetic theory of the growth of vapor bubbles in the liquid phase and the transitions are then associated with the existence of a thermodynamic barrier to the formation of a droplet or cluster of the gas phase in a homogeneous metastable parent phase of the liquid. Once a bubble overcomes the barrier and grows beyond the critical radius, the bubble expands spontaneously to macroscopic size. Volmer and Weber (1926) assumed that the rate of nucleation is proportional to the probability of formation of clusters of critical size and therefore the rate of nucleation is proportional to $\exp(-\Delta W^*/kT)$, ΔW^* being the free energy of formation of a critical cluster and k is the Boltzman constant, and T is the temperature in K. A more complete kinetic approach to nucleation was initiated by Farkas which served as a basis for subsequent treatments of Becker and Doring (1935), Zeldovich (1943) and Frenkel (1946). In the classical theory of homogeneous nucleation, largely based on the treatment of Becker and Doring, the nucleation

rate is calculated on the basis of a population balance for the size distribution of clusters generated by condensation and evaporation of atoms onto and from the clusters. The so called "classical" nucleation theories such as that of Becker and Döring (BD), generally consider the rate of phase transformation of metastable states as a function of the degree of metastability.

In the theory of homogeneous nucleation or cavitation from the liquid, clusters or "embryos" of the gas phase are regarded as spherical cavities having macroscopic properties such as surface tension, even though they may contain less than 100 molecules. The total work to form a cluster of n molecules is assumed to be given by (Blander and Katz, 1975)

$$W = \sigma A - (P_G - P_L) V_G + x(\mu_G - \mu_L) \quad (2.1)$$

where P_G is the pressure of the gas in the bubble, P_L is the pressure of the surrounding liquid, V_G is the volume of the bubble, x is the number of molecules vaporized into the cavity, μ_G and μ_L are the chemical potentials of gas and liquid respectively. The first term is due to the surface tension, σ , and A is the surface area of the cluster. For a spherical cluster, $A = 4\pi r^2$. In Equation (2.1), since the first term is positive and normally $P_G > P_L$ and $\mu_G < \mu_L$, there exists a maximum of the work function, W_c , at which the cluster has the critical size with a radius of r_c .

The second approach is based on equilibrium theory. This theory, in contrast with theories of the nucleation type,

predicts a quite definite value of the tensile strength of a liquid at any temperature. This value is that of the negative pressure ordinate corresponding to the minimum of the van der Waals isotherm and is given by the condition $(\partial P/\partial V)_T=0$.

EQUATION OF STATE OF LIQUIDS

The Van Der Waals Theory of Liquids

Modern theories of the relation between intermolecular forces and the properties of fluids can probably be traced to two fundamental studies, one experimental and the other theoretical, reported a century ago. In 1869, Andrews presented a set of measurements of the equation of state of carbon dioxide in which he showed that it was possible to pass from the vapor to the liquid state without a noticeable change in phase. This process can be carried out by suitable changes in the thermodynamic state of the system. Thus, if a gas is heated at constant volume until it is above some critical temperature, T_c , compressed, and then cooled to the starting temperature it is found that the resulting fluid has all the properties of a liquid.

The second advance was primarily theoretical work done by van der Waals in 1873. His approach was to develop an explicit description of the equation of state so that the pressure of the system was given by the equation where V is the volume of the fluid and T its temperature. The van der Waals theory gave an expression for $P(V,T)$ that

$$\left(p + \frac{N^2 a}{V^2}\right)(V - Nb) = NKT \quad (2.2)$$

depended on two parameters, a and b , to be determined from experimental data. The theory is rather simple to describe and does not tell us very much about the fundamental structure of dense fluids. Nevertheless, it represents probably the first successful description of the macroscopic properties of a fluid in terms of molecular properties.

From the point of view of describing the properties of a liquid in terms of the properties of its constituent particles, parameters a and b are of particular interest. Van der Waals argued that two properties of molecules give rise to the gas-liquid phase change, namely, the strongly repulsive forces found when the molecules are close together and the weaker attractive forces found when the molecules are further apart. If the liquid is at a relatively high temperature the repulsive forces acting between the molecules imply that the volume of the system cannot be reduced below some limiting volume Nb . However, van der Waals also recognized that the attractive forces between the molecules are important at lower temperatures. He argued that these attractive forces would increase the pressure acting on the molecules and hence the term $N^2 a/V^2$ was added to the ideal gas equation $pV = NKT$. Thus van der Waals equation recognizes both attractive and repulsive intermolecular interactions.

The van der Waals equation also gives a good qualitative description of the Andrews isotherms which are the P-V curves for given temperatures. In particular, it predicts the existence of a critical point, and this can be found by using the fact that at this point there is a point of inflection on the P-V isotherm

$$\frac{\partial p}{\partial V}=0, \quad \frac{\partial^2 p}{\partial V^2}=0 \quad (2.3)$$

Using these conditions it is found that

$$P_c = \frac{a}{27b^2}; \quad T_c = \frac{8a}{27bK}; \quad V_c = 3Nb \quad (2.4)$$

By substituting the critical pressure $P_c = 3.3978 \text{ MPa}$ and $T_c = 126.193 \text{ K}$ one could obtain the Andrews isotherms for liquid nitrogen. For the temperatures $T = T_c, 110, 95, 85, 77, 67 \text{ K}$, we plot P-V curves as shown in Figure 1. At temperatures less than T_c the P-V isotherms predicted by the van der Waals equation rise steadily from zero, at large V, cross the coexistence curve, and then reach a maximum. The isotherms then fall to some minimum value and rise rapidly, crossing the liquid side of the coexistence curve before going to very high pressures at small volumes.

The tensile strength defined from the van der Waals equation is the vertical distance P_T from the minimum point of the P-V curve for given temperature to the horizontal axis .

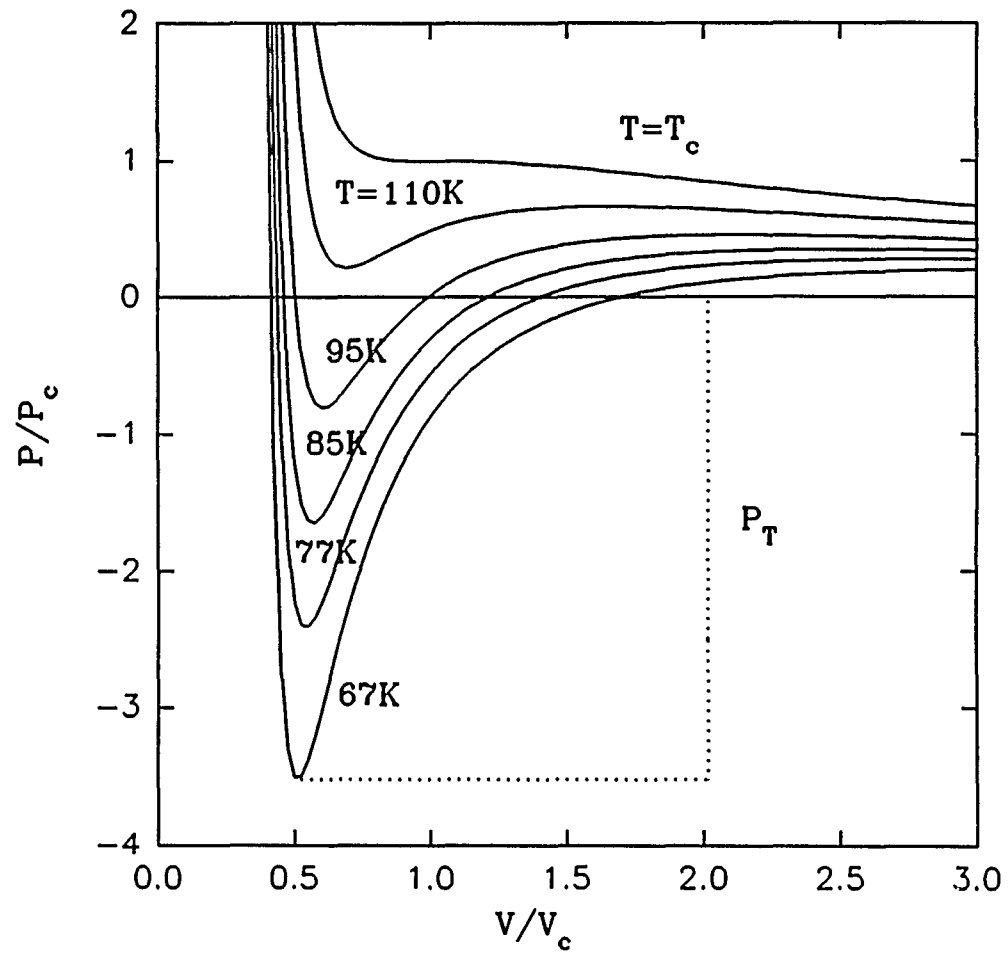


Figure 1. Andrews isotherms of liquid nitrogen for $T_c, 110, 95, 85, 77, 67$ K.

The tensile strength of liquid nitrogen can be plotted against the temperature as shown in Figure 2.

The van der Waals equation exhibits the loop as shown in Figure 3 along any isotherm with $T < T_c$. At point A, the system is in the stable liquid phase. If the volume is increased slowly and isothermally in such a way that the liquid remains in equilibrium, the pressure of the liquid will monotonically decrease until point B is reached on the liquid saturation curve. By continuing expansion of the system at equilibrium, vapor will be formed and will coexist in stable equilibrium with the liquid. The curve, BF, along which the liquid and vapor coexist, is found by means of the Maxwell construction. The construction is formed by requiring equal areas under the curves BCD and DEF. The molar fraction of vapor is determined by the position along BF. The physical meaning of this requirement is that the work done to form vapor phase from liquid phase is reversible. At point F, the vapor saturation curve is reached and system consists entirely of vapor.

There are two main differences between the van der Waals equation and experimentally determined Andrews isotherms. The first is the behavior of the fluid within the region bounded by the coexistence curve. Experimentally, much of this region is inaccessible although the mechanically unstable superheated liquid can be thought of as representing the fluid state in part of this region. The van der Waals

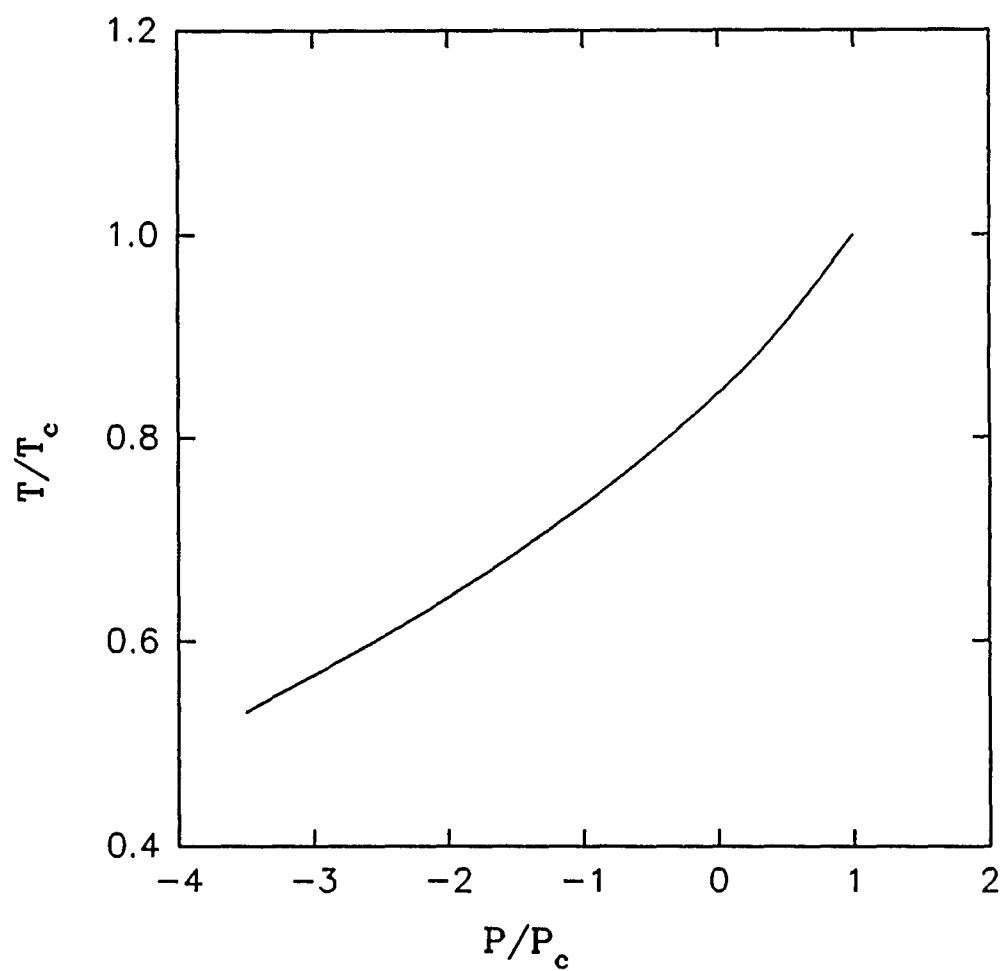


Figure 2. The tensile strength of liquid nitrogen predicted from the van der Waals equation as a function of the temperatures.

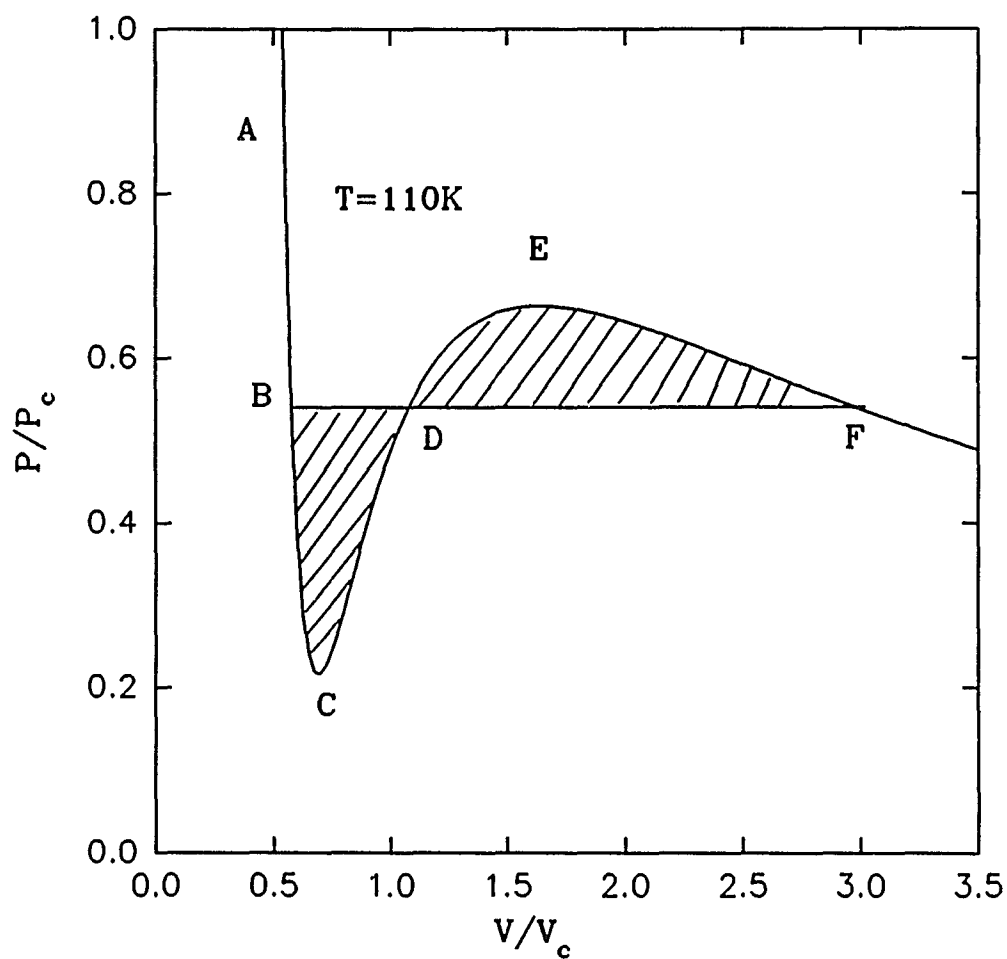


Figure 3. P-V curve for $T=110\text{ K}$. The areas of the shaded region BCD and DEF are equal.

equation is continuous through this region and has to be supplemented with thermodynamic calculations before it predicts the discontinuous gas-liquid transition. In addition, the negative value of the compressibility, $(\partial P/\partial V)_T$, (CDE in Figure 3) in the two phase region is not found experimentally. The second major difference between the behavior of real fluids and the van der Waals equation, which cannot be seen from the figure, is the qualitatively different behaviors of the experimental and theoretical critical isotherms.

Briefly, it is found that the van der Waals equation gives an incorrect mathematical description of the way in which the fluid approaches the critical point. A good example is the way in which the densities of the gas and liquid tend to the critical density as the two fluid phases approach this point along the coexistence curve. The van der Waals equation predicts

$$\rho_l(T) - \rho_g(T) = B(T_c - T)^\beta \quad (2.5)$$

where the index $\beta=0.5$, ρ_i is the density of phase i , and B is some constant. Experimentally, it is found that $\beta=0.30-0.37$. It can be shown that if the Helmholtz free energy, A , is an analytic function of V and T everywhere, then a Taylor expansion of A in powers of $V-V_c$ and $T-T_c$ gives $\beta=0.5$. Consequently, the experimental measurements suggest that the free energy of a fluid is not an analytic function of V and T in the neighborhood of the critical point. It is now

well established that real fluids do not follow the van der Waals equation near the critical point.

Since the van der Waals equation has been proved to be invalid when temperature is either close to 0 K (Maris and Xiong) or near the critical temperature T_c and the CDE portion of the P-V curve predicted from van der Waals equation has never been found, it is questionable if the tensile strength defined as in Figure 2 is valid. Temperley and Trevena (1977) showed that the metastable region disappears if it were possible to make a true equilibrium calculation of the equation of state of a real liquid. Therefore it would seem that an equation of state with a van der Waals loop (BCDEF in Figure 3) is not correct as an equilibrium consequence of a model. For a system including a large number of particles, the isotherm should consist two disconnected portion connected by a horizontal line BF as shown in Figure 3. The effect of an attractive intermolecular interaction whose range is gradually lengthened has investigated by Kac, Uhlenbeck et al (1963). They find that the van der Waals loop disappears, giving, below the critical temperature T_c , an isotherm like ABDF as shown in Figure 3 if three limiting processes are involved - making the range of the interaction large, making its strength small and making the number of the particles large.

In order to describe the imperfect gas and liquids more rigorously, it is necessary to modify the equation of state of a liquid. If the interaction between molecules of a real gas

or liquid is known, its equation of state can be expressed as a virial series. The magnitude of the theoretical tensile strength of the liquid is very different from that which is predicted from the van der Waals equation.

The Tensile Strength Calculated from the Virial Series

Generally, the equation of state of a liquid can be expressed as a virial series

$$P = \frac{NKT}{V} + \frac{B_1}{V^2} + \frac{B_2}{V^3} + \frac{B_3}{V^4} + \dots \quad (2.6)$$

where B_1, B_2, B_3 , etc. arise respectively from configurations in which two, three, four, etc. molecules are near one another. The tensile strength of the liquid is defined as the pressure amplitude when an abrupt change in P-V curve occurs. Unfortunately, it becomes very difficult to calculate virial coefficients for terms higher than V^5 in the equation of state, even if it is assumed that only pairwise additive interactions are important. Except for the special case of the Gaussian model, where terms up to twelfth virial coefficient have been obtained analytically, and for hard spheres, where coefficient up to the seventh have been reported. Exact results for the first seven virial coefficients for hard spheres have been reported by Ree and Hoover (1967) as shown in Table 1.

If one rewrites the van der Waals equation in virial form by using the identity $\frac{1}{1-b\rho} = 1 + b\rho + (b\rho)^2 + (b\rho)^3 + \dots$ then

$$P + ap^2 = KTp (1 + bp + b^2p^2 + b^3p^3 + \dots) \quad (2.7)$$

where $\rho = N/V$, N is the number of particles in the system and V is the volume.

By using the coefficients $a = 3.76838 \cdot 10^{-49}$, $b = 6.40909 \cdot 10^{-29}$ determined from Equation (2.4) and $\sigma = 3.3 \text{ \AA} = 3.3 \cdot 10^{-10} M$ where σ is the diameter of a molecule, one could get two different equations of state and they show a progressive discrepancy with increasing density or decreasing temperature. As we might expect, the van der Waals equation is valid only when the temperature of the liquid is very high or the density is extremely low. Therefore, if the virial form of the equation of state can better describe the liquid, then the theoretical tensile strength predicted by the van der Waals equation does not represent the true value of the liquid. Unfortunately, the virial form of equation of state cannot describe the behavior of a liquid in the phase transition region satisfactorily and predict the correct tensile strength of the liquid. The reasons are as follows. In practice, one has to truncate the virial series to get a usable expression for the equation of state. If one does not keep infinitely many terms of the virial series, he can never see the "flat isotherm" nor the abrupt change of pressure for any value of volume, so that one could not predict where the phase transition occurs. The tensile strength of the liquid cannot be predicted quantitatively. For example, if we keep the first eight terms

TABLE I
HARD SPHERE VIRIAL COEFFICIENTS

Virial Coefficients B_i	Values
B_2	$(2\pi/3) \sigma^3 = b$
B_3/b^2	0.625
B_4/b^3	0.2869
B_5/b^4	0.1103 ± 0.0003
B_6/b^5	0.0386 ± 0.0004
B_7/b^6	0.0127
B_8/b^7	0.0040

of the virial series, the pressure P decreases monotonically with increasing volume and no "flat isotherm" exists. Furthermore, P can never be negative since all of the virial coefficients are positive for the hard sphere model.

When a infinite system consisting of a very large number of particles is considered, the above difficulty of finding the "flat isotherm" might be removed. With the help of modern computer techniques one can construct a polynomial consisting of a large number of terms, with a change of slope sufficiently abrupt as to appear discontinuous in P - V curve (Croxtton 1975). However, it will be unlikely to obtain a definite value of the theoretical tensile strength for an acoustic cavitation experiment in which an intense acoustic field is rapidly focused into such a small volume that the

number of particles is not large enough to satisfy the requirement to obtain the "flat isotherm".

Using the truncated virial series to calculate the thermodynamic properties appears to be invalid as follows. First, little information is available on the radius of convergence of the virial expansion and there is no guarantee that this approach will work even if a large number of terms in the series is available. Second, in the region of phase transition, various thermodynamic quantities are no longer analytic functions of the state variables. A number of studies of the truncated virial series have been carried out, the most extensive being that of Barker and Henderson (1967) on gas-liquid transition. They showed that a five-term virial expansion gave reasonable results at temperatures down to the critical temperature and to densities somewhat higher than the critical density. However, the truncated expansion does not give very good results in the liquid region.

The *Padé* approximation to an infinite series provides a reasonably accurate analytic expression for the low to intermediate-density equation of state of a nonideal gases and liquids though it does not afford much physical insight into the problem of phase transitions. The *Padé* approximation of the equation of state is written in the form of

$$\frac{PV}{NKT} = 1 + \frac{bp(1 + 0.063507bp + 0.017329b^2p^2)}{1 - 0.561493bp + 0.081313b^2p^2} \quad (2.8)$$

for the hard sphere model of a liquid. Xiong and Maris (1991)

used this as the starting point to postulate their analytic expression of speed of sound as a function of pressure in liquid helium. However, the P - ρ curve (pressure versus density of the liquid) derived by them is continuous throughout the phase transition region. If one converts their P - ρ curve to a P - V curve, no "flat isotherm" corresponding to the phase transition can be found. Thus, Xiong and Maris' model cannot fit into the existing models obtained from the equation of state. Although they obtained the negative pressure at the phase transition point, the value is similar to that estimated from the van der Waals equation.

Theoretically one could possibly use the equation of state to calculate the tensile strength of a liquid. However, in practice, the value of the calculated tensile strength depends upon the number of terms of the truncated infinite series form of the equation of state and it is difficult to estimate the radius of convergence of the infinite series. We therefore are not going to use the equation of state to estimate the tensile strength of liquid nitrogen at the present stage. We now turn our attention to the second approach, that is, the kinetic theories of homogeneous nucleation.

KINETIC THEORIES OF HOMOGENEOUS NUCLEATION

The kinetic theories of homogeneous nucleation in liquids are based on the calculation of the rates of bubble formation

in a liquid. In this section we will discuss the physical origins of the so called drop model and the predicted classical nucleation rates based on this model. We will show, as is well known, that the predicted nucleation behavior is very sensitive to the choice of the thermodynamic parameters of the microcluster assumed in the drop model. Next, we discuss various modifications of the theory of homogeneous nucleation.

We start with the fundamental equation of homogeneous nucleation that is, the homogeneous nucleation rate, J , is given by the expression

$$J = \frac{\sum_{i=0}^{\infty} i^2 \alpha_i \beta_i}{\int_0^{\infty} \left[\sum_{i=1}^{\infty} \frac{1}{n(x) s(x)} \right]^{-1} dx} \quad (2.9)$$

where $n(x)$ is the number of clusters or bubbles per unit volume containing x molecules, $s(x)$ is their surface area which is given by $s(x) = 4\pi r_i^2$, α_i is the sticking coefficient which is about equal to 1, β_i is the rate of arrival of an i -mer at a unit area per unit time, and the summation extends over all species present in significant concentrations. Note that here we summarize forming rates of all kinds of bubbles that contain 1, 2, 3, ..., ∞ molecules.

It should be made clear here that we are considering polymers or clusters in two different senses. The i -mers are small polymers which enable us to simply express nonidealities

of the gas. The "x-mers" are droplets or bubbles and in the theory only those near critical size drops or near critical sized bubbles which contain x monomer units are significant.

The number of bubbles containing x molecules formed in the thermodynamic equilibrium is given by

$$n(x) = N \exp[-W(x)/kT] \quad (2.10)$$

where N is the total number of monomers per unit volume and $W(x)$ is the reversible work to be done to form a bubble with x molecules and given by Equation (2.1).

When the density fluctuation in a liquid due to the external condition changes is large enough, the vapor bubble, if it exceeds the critical size, will grow and homogeneous nucleation occurs. When the bubble reaches the critical size, the chemical potentials of the bubble and surrounding liquid phase are equal to maintain the unstable equilibrium, i.e.

$$\mu_G(P_G) = \mu_L(P_e) \quad (2.11)$$

where P_e is the equilibrium ambient pressure.

On the other hand, the pressure dependence of the chemical potential can be obtained from the differential form

$d\mu = -sdT + v dP$, by integrating at constant temperature from pressure P_e to P_L

$$\mu_L(P_L) - \mu_e(P_e) = \int_{P_e}^{P_L} V_L dP = \int_{P_e}^{P_v} P_G V_G d \ln P \quad (2.12)$$

or

$$\mu_L - \mu_e = kT \ln \frac{P_v}{P_e} \quad (2.13)$$

where P_L and P_e are the pressures of liquid and gas phase in equilibrium respectively. V_L and V_G are volume of liquid and vapor respectively.

From Equation (2.12), one can easily get

$$V_L (P_L - P_e) \approx P_e V_G \ln \left(\frac{P_v}{P_e} \right) = P_e V_e \ln \left(\frac{P_v}{P_e} \right) \quad (2.14)$$

where V_e is the volume of a mole of gas at equilibrium with the stable liquid. Since $P_e \approx P_v$, $P_v/P_e = 1 - (P_v - P_e)/P_e \approx 1$. Expanding the logarithm and keeping terms up to second order, one obtains an expression for the correction factor δ :

$$\begin{aligned} \delta &= \frac{P_v - P_L}{P_e - P_L} = 1 - \frac{V_L}{V_e} + \frac{1}{2} \left(\frac{V_L}{V_e} \right)^2 \\ &= 1 - \frac{d_G}{d} + \frac{1}{2} \left(\frac{d_G}{d} \right)^2 \end{aligned} \quad (2.15)$$

The above expression is valid for $P_v \approx P_e$. Equation (2.15) relates the pressure inside the vapor bubble to the equilibrium vapor pressure of the system and the proportional constant δ is called the Poynting correction. The reason for converting the pressure inside the critical bubble, P_v , is as follows. The pressure inside the critical bubble is equal to the vapor pressure of the liquid at a total hydrostatic pressure equal to the ambient pressure P_L .

However, the equilibrium vapor pressure P_e is what we measure on a liquid under a hydrostatic pressure equal to its vapor pressure.

To obtain the final expression for the rate of homogeneous nucleation, one has to know the capture rate β_i . It can be approximated by assuming that the capture rate is obtained simply from the collision rate between the bubble and background liquid:

$$\beta_i = P_L / (2\pi mkT)^{1/2} \quad (2.16)$$

By assuming that the pressure in the bubble, P_G is equal to the vapor pressure P_V and notice that when the bubble reaches the critical size, the bubble surface is in mechanical balance. The pressure inside the bubble can be obtained from Laplace-Kelvin's equation

$$P_V = P_L + \frac{2\sigma}{r_c} \quad (2.17)$$

Bubbles smaller than the critical tend to collapse, and bubbles larger than the critical tend to continue to grow spontaneously. Since bubbles can grow to critical size only from subcritical sizes which tend to collapse, one need only to consider those close to mechanical equilibrium and their pressure can be approximated by

$$P_G = P_L + \frac{2\sigma}{r} \quad (2.18)$$

where σ is the surface tension of the bubble and r_c is the critical radius of the bubble. In such a case, one can expand

the work function $W(x)$ around the critical radius r_c and get

$$W \approx \frac{4}{3} \pi r_c^2 \sigma - 4 \pi \sigma [r - r_c]^2 B + \dots \quad (2.19)$$

where, for mechanical equilibrium only

$$B \approx 1 - 1/3 (1 - P_L/P_V) \quad (2.20)$$

If $P_L \ll P_V$, the factor $B \approx 2/3$ this is for the superheating case. On the other hand, if $r = r_c$, the factor B does not appear in the Equation (2.19) and it is equivalent to $B = 1$, for the case of stretching the liquid.

Following the derivation made by Blander and Katz (1975), one can obtain the final form of the nucleation rate

$$J = N \left[\frac{2\sigma}{\pi m B} \right]^{1/2} \exp \left[\frac{-16 \pi \sigma^2}{3 k T [P_V - P_L]^2} \right] \quad (2.21)$$

where m is the molecular mass.

Expressing the result in terms of common laboratory units, one obtains

$$J \approx 3.73 \cdot 10^{35} \left[\frac{d^2 \sigma}{M^3 B} \right]^{1/2} \exp \left[\frac{-1.182 \cdot 10^5 \sigma^3}{T [P_V - P_L]^2 d^2} \right] \quad (2.22)$$

where $B \approx 1$, for the case of cavitation and the units are $J(\text{cm}^{-3} \text{sec}^{-1})$, $P_V(\text{atm})$, $P_L(\text{atm})$, $T(\text{K})$, $\sigma(\text{erg cm}^{-2})$, $d(\text{g cm}^{-3})$, $M(\text{g mole}^{-1})$.

In Equation (2.21), the preexponential terms vary very slowly with temperature. However, any temperature change inside the exponential will have a very strong effect on the

rate of nucleation. The predicted nucleation rate is even sensitive to the changes of the surface tension σ and the pressure in the liquid. Thus, to obtain accurate expressions for surface tension and the pressures in the exponential terms is crucial to the studies of the tensile strength of liquids.

The surface tension of liquid nitrogen for wide temperature ranges has been studied extensively (Baidakov et. al. 1982a, 1982b, Jacobsen et. al. 1986). The surface tension of liquid nitrogen can be described by the equation (Baidakov et. al. 1982a)

$$\sigma = \sigma_M (1 - \tau)^{\mu_1} (1 + m\tau) \quad (2.23)$$

where τ is the reduced temperature $\tau = T/T_c$ and

$$\sigma_M = 26.82 \cdot 10^{-3} \text{ N M}^{-1}$$

$$m = 0.170$$

$$\mu_1 = 1.274$$

We compared this expression with some of the reported surface tension values in the temperature range from 78 K to 120 K and found they are in good agreement with the experimental results (within five percent).

To calculate the rate of homogeneous nucleation, the equilibrium pressure of the vapor phase, P_e also need to be determined. There have been many careful measurements of the equilibrium vapor pressure of liquid nitrogen. One of the extensive studies on this subject was carried out by Wagner

(1973). He measured the equilibrium pressure of liquid nitrogen in the temperature range from 63 K up to the critical point. The pressure equation determined can be written as

$$P_e = \exp(P_c * [T_c T^{-1} (n_1 \tau + n_2 \tau^{1.5} + n_3 \tau^3 + n_4 \tau^6)]) \quad (2.24)$$

$\tau = 1 - \frac{T}{T_c}$ and coefficients in Equation (2.24) are given as

$$n_1 = -6.102549344$$

$$n_2 = 1.153658492$$

$$n_3 = -1.087810693$$

$$n_4 = -1.755769179$$

The more complete summary of different measurements of equilibrium vapor pressure of liquid nitrogen is carried out by Jacobsen (1986) and the functional form for the vapor pressure equation is

$$\frac{P}{P_c} = \frac{T}{T_c} (1 + N_1 \tau + N_2 \tau^{1.9} + N_3 \tau^2 + N_4 \tau^{2.4} + N_5 \tau^3 + \sum_{i=6}^{17} N_i \tau^{(i+1)/2}) \quad (2.25)$$

where $\tau = [(T_c/T) - 1]$. P_c and T_c are the critical pressure and temperature, respectively. Coefficients for Equation (2.25) are given in Table II.

Those coefficients that do not appear in the Table II are zero. For calculating the Poynting Correction δ in the Equation (2.22), it is necessary to have the function form of densities for both liquid and vapor phase of nitrogen. The saturated vapor density of nitrogen as a function of

TABLE II
COEFFICIENTS FOR LIQUID-VAPOR COEXISTENCE EQUATION OF
NITROGEN

$N_1 =$	-5.072183802
$N_2 =$	$0.1367990776 \cdot 10^2$
$N_4 =$	$-0.1194002133 \cdot 10^2$
$N_6 =$	2.641788428
$N_{10} =$	-0.3781265428
$N_{13} =$	$0.7593697713 \cdot 10^{-1}$

temperature is

$$\ln \frac{\rho_G}{\rho_c} = \sum_{i=1}^{23} N_i \tau^{(i+1)/3} + N_{24} \ln \theta + N_{25} \tau^{0.325} \quad (2.26)$$

and saturated liquid density equation is

$$\frac{\rho_L}{\rho_c} = 1 + \sum_{i=1}^{23} N_i \tau^{(i+1)/3} + N_{24} \tau^{0.325} + N_{25} \ln(\theta) \quad (2.27)$$

where ρ_L is the density of the saturated liquid and $\rho_c = 11.177 \text{ mol/dm}^3$. Table III and IV give the coefficients for Equation (2.26) and (2.27) respectively.

So far we have obtained all of the necessary parameters in Equation (2.22). For a given temperature one is able to determine the Poynting correction knowing the saturated liquid and vapor density, and the surface tension is calculated from Equation (2.23). We plotted both saturated vapor and liquid density as shown in Figure 4.

Substituting all of the necessary parameters into Equation (2.22) and rearranging it, one can obtain an analytic expression of pressure in the liquid as a function of

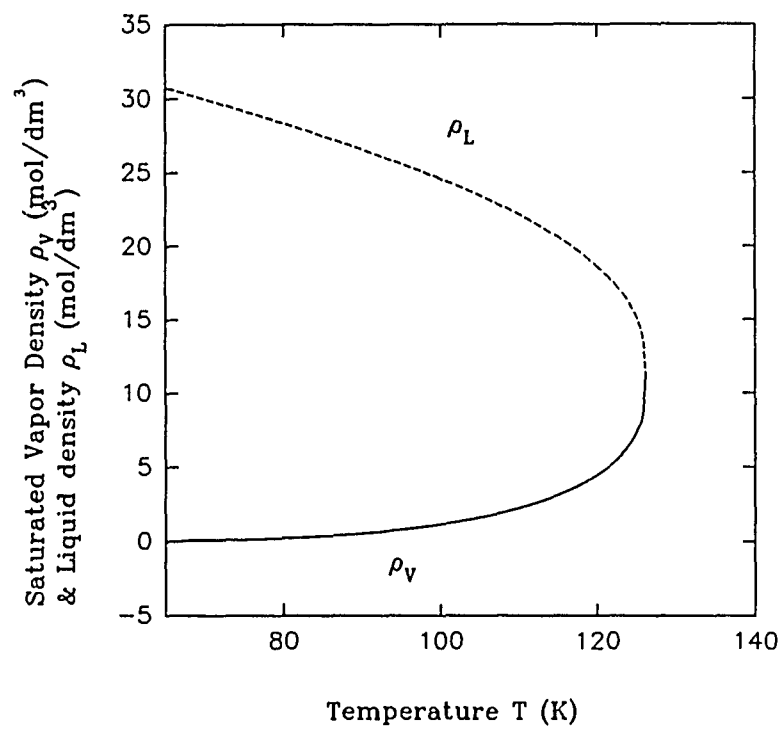


Figure 4. The saturated vapor and liquid densities of nitrogen vs. temperature.

TABLE III
COEFFICIENTS FOR SATURATED VAPOR PRESSURE EQUATION

$N_1 = 0.1780437699 \cdot 10^2$
$N_3 = 0.1202958313 \cdot 10^4$
$N_4 = -0.4601087081 \cdot 10^4$
$N_5 = 0.1051265347 \cdot 10^5$
$N_6 = -0.1188582325 \cdot 10^5$
$N_8 = 0.1740923806 \cdot 10^5$
$N_9 = -0.1934202934 \cdot 10^5$
$N_{10} = 0.7191464655 \cdot 10^4$
$N_{24} = 0.8015275202$
$N_{25} = -0.1895717510 \cdot 10^3$

TABLE IV
COEFFICIENTS FOR LIQUID DENSITY EQUATION

$N_1 = 1.345167397$
$N_2 = 0.2721335451 \cdot 10^2$
$N_3 = 0.1189562787 \cdot 10^3$
$N_4 = -0.2681972897 \cdot 10^3$
$N_5 = 0.3292110413 \cdot 10^3$
$N_6 = -0.1381052419 \cdot 10^3$
$N_{10} = 0.3447426258 \cdot 10^2$
$N_{24} = -0.5724027229 \cdot 10^2$
$N_{25} = -1.592975033$

temperature for different nucleation rates. We plotted P_L for nucleation rates of $J=1$, 10^6 , 10^{11} , and 10^{22} (bubbles $\text{cm}^{-3} \text{sec}^{-1}$) as shown in Figure 5. Also indicated is the coexistence curve of nitrogen.

Equation (2.21) or (2.22) serves as the fundamental equation that is used to calculate the tensile strength of liquid nitrogen. We will primarily be concerned in this dissertation with the negative pressure region of the nucleation curve and we will compare our measured pressure

amplitude in liquid nitrogen with results obtained from Equation (2.22), i.e. Figure 5. The reason is that Equation (2.22) has been proven experimentally by Sinha (1982, 1987) in the positive pressure region.

At this point, we reexamine in more detail some basic assumptions and drastic approximations in the derivation of Equation (2.21). First, to obtain Equation (2.14), one has to assume that the vapor bubble behaves as an ideal gas and the liquid phase is incompressible (when the vapor phase is nonideal then a correction factor needs to be introduced and we will discuss it later). Then one can get

$$P_L = P_e + \frac{KT}{V_L} \ln(P_G/P_e) \quad (2.28)$$

where V_L is the molecular volume of the gas phase. The validity of this approximation has no proof. Furthermore, one has to relate the pressure in the bubble to the physically measurable quantities as described in Equation (2.15) based on the assumption that $P_V \approx P_e$, i.e. the pressure in the vapor bubble is very close to the equilibrium vapor pressure at interface of bulk liquid and vapor phase. Again this is not justified. Blander et al. (1973) showed that the Poynting correction is given by

$$\delta = 1 - P_e(T)M/(d_L)RT \quad (2.29)$$

where M is the molecular weight and R is the gas constant in units of $\text{cm}^3 \text{ atm mole}^{-1} \text{ deg}^{-1}$. If P_L is very close to P_e ,

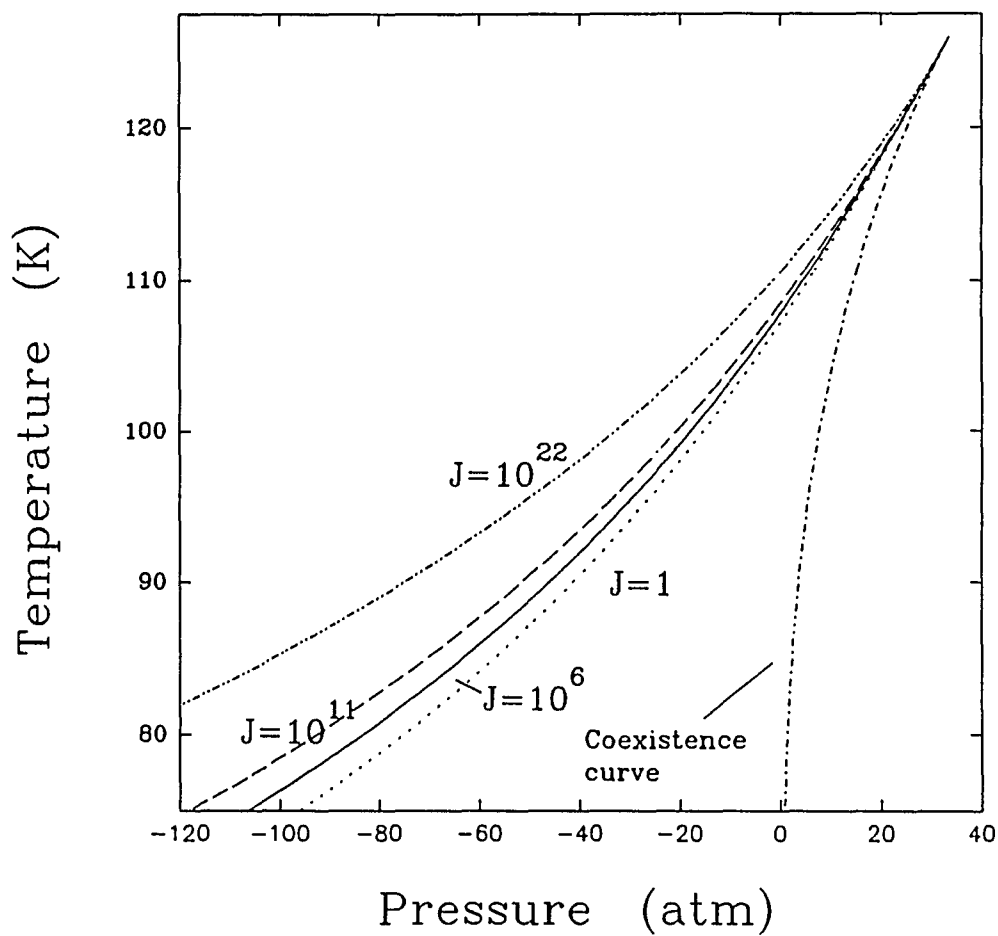


Figure 5. The pressure in liquid nitrogen vs. temperatures for different nucleation rates.

δ should be very close to 1. We plot δ against the temperature in the liquid and indeed as shown in Figure 6 from the temperature lower than 100 K, δ is very close to 1.

Based on $P_G \approx P_e$, one can also derive the familiar form of generalized Laplace-Kelvin equation

$$P_G = P_e \exp\left(-\frac{2\sigma V_L}{kT r}\right) \quad (2.30)$$

Secondly, a crude approximation made is that the surface tension of the bubble is replaced by the interfacial surface tension between the bulk liquid and its saturated vapor phase. The biggest controversy of the classical theory of homogeneous nucleation has been around this assumption. As one can see, the classical nucleation theory is far from perfect and we will discuss some different approaches in the next section.

From the analysis of this section, we conclude that neither the van der Waals equation nor the virial form of the equation of state with finite number of terms can predict the tensile strength correctly. In the derivation of the classical nucleation theory, since not only the interactions between the nearest molecules are considered, the long range interactions are also take into account (see Equation (2.9)). Temperley et. al. (1977) showed that the kinetic nucleation theory is compatible with the equilibrium approach, or the equation of state if an infinite number of terms are included. One should expect similar results of calculated tensile strength from either approach.

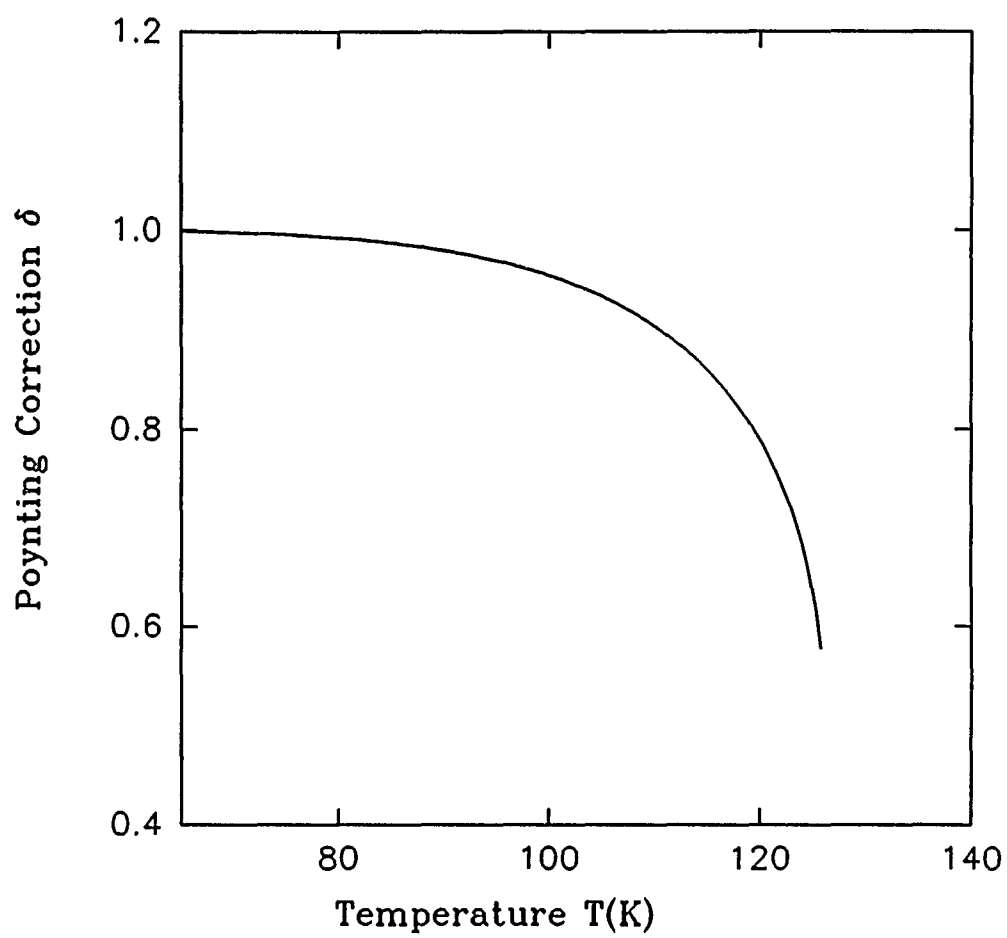


Figure 6. Poynting Correction vs Temperatures.

THE MODIFICATION OF CLASSICAL NUCLEATION THEORY

The first modification of the classical nucleation theory comes from the studies of the condensations of vapor by Lothe and Pound (1962). They pointed out that the classical expression of Equation (2.10) needs a correction factor. The reason for the correction factor is as follows. When a liquid droplet is in the vapor phase, it can move around freely. In contrast, while it is in the liquid phase, its translational motion is limited. The second difference is the rotation. Lothe and Pound reasoned that the droplet in the vapor could rotate freely, while the rotational motion is constrained and is only limited to small local oscillations in the liquid. In other words, both the translational and the rotational degrees of freedom are released as the droplet is transferred from the liquid phase to the vapor phase. Based on these ideas, Lothe and Pound estimated that the numerical value of the correction factor is about 10^{17} .

Compared with experimental results, Lothe and Pound found that liquid drop nucleation could be divided into two classes: those liquids which obeyed the classical theory and those which obeyed the Lothe-Pound theory. These two classes of liquids are called "classical" liquids and "Lothe-Pound" liquids, respectively. For the liquid-vapor phase transition, there is similar argument. However, Lothe-Pound theory is controversial because the reasoning is not convincing. Reiss et al. (1968) argued that the Lothe-Pound treatment is invalid

because it doubly counts certain contributions to the free energy, and with their correction, they find a result close to what the classical theory predicted.

There have been many different theories of homogeneous nucleation proposed recently (Bezverkhii et al. 1986, Oxtoby 1989, Nowakowski et al. 1990, Dillmann et al. 1990, Girshick 1991, G.Shi et al. 1990). Mainly they can be classified into two categories. The first kind is the "conventional approach" in which the traditional macroscopic parameters of a liquid such as surface tension are used (Bezverkhii et al. 1986, Girshick 1991, G.Shi et al. 1990). The modified expression for the rate of homogeneous nucleation is different from the classical expression by a multiplication factor e^{θ}/S , where S is supersaturation and $\theta = (\sigma s_1/kT)$, σ is surface tension, and s_1 is monomer surface area. Values of θ for various substances and temperatures range from about 3 to 50. The second kind is the "nonclassical approach" in a different sense from the previous one (Oxtoby 1989, Nowakowski et al. 1990, Dillmann et al. 1990). In these approaches, they avoid the use of the surface tension and instead the microscopic molecular interaction potential is employed. The predicted nucleation rate from this approach is greatly dependent upon the choice of the interaction potential. Most of the predicted nucleation rates are also higher than those calculated from the classical theory of homogeneous nucleation and can be different by a factor of 10^{10} to 10^{20} . Only Oxtoby

(1989) predicted that for certain kinds of interaction potentials the nucleation rates can be lower than those calculated from the classical homogeneous nucleation theory.

Although there are many controversies surrounding the basic assumptions and a lot of attempts to improve upon it, the classical nucleation theory remains as the most widely accepted method to predict nucleation behavior of real substances at least in a qualitative correct manner. For the tensile strength of liquid nitrogen, the approaches different from the classical theory predict lower values. The tensile strength of liquid nitrogen for $J=10^{17} \text{ cm}^3\text{sec}^{-1}$ calculated from those nonclassical theories is equivalent to that which is predicted from the classical theory for $J=1 \text{ cm}^3\text{sec}^{-1}$. However, one can see from Figure 5 that the predicted negative pressure is not substantially different, less than 30 percent. Unless one can determine the pressure very accurately, he cannot tell the difference in real measurements.

CHAPTER III

DETERMINATION OF PRESSURE IN A LIQUID

There are basically two different approaches reaching the homogeneous nucleation limit of a liquid. The first one is superheating the liquid under a constant pressure where the temperature of the liquid is raised rapidly to a critical value at which homogeneous nucleation occurs. In a graph of temperature versus pressure, it follows a vertical path to reach the homogeneous nucleation curve. The other approach is to measure the tensile strength of the liquid. It follows a horizontal path, changing the pressure in the liquid under constant temperature and stretching the liquid until it breaks. The superheating experiments are more common in studying homogeneous nucleation in liquids but they are limited to the positive pressure region and therefore one can only test the nucleation theory over a narrow range of temperatures and pressures. A large part of the homogenous nucleation curve lies in the negative pressure region and is only accessible by the measurement of the tensile strength.

To measure the tensile strength of liquid nitrogen, it is essential to correctly determine the pressure amplitude of a focused acoustic field in the liquid. The difference of the equilibrium vapor pressure amplitude and the ambient pressure,

i.e. the pressure amplitude in the surrounding liquid, is the tensile strength. The existing methods to determine the pressure amplitude include Debye's theory, solving the KZK (Khokhlov-Zabolotskaya-Kuznetsov) equation, and light diffraction. Debye's theory gives the expression of the pressure at the focus as a function of the dimensional parameters of a focused concave spherical transducer and the frequency. The KZK equation is an ordinary differential equation for the pressure distribution. For given boundary conditions the pressures at the focal plane and along the acoustic axis can be determined for the fundamental frequency and the higher harmonics. Debye's theory and solutions to the KZK equation are valid restrictively to the concave spherical transducer with small aperture angle. To determine the pressure amplitude at the focal region of the transducer by these two methods, one has to first use an equivalent circuit model to determine the pressure amplitude at the surface of the transducer. Neither Debye's theory nor the KZK equation is valid for transducers with large aperture angle such as a hemispherical transducer. The third method, light diffraction, is well established (Sliwinski, 1990, Kwiek, 1989, Abeele, 1990, Reibold, 1976) for the measurement of the acoustic pressure of a planar ultrasonic wave. However, the ability to do a similar measurement in case of spherical waves has been questioned. Nagai (1986) pointed out that the Raman-Nath theory, even for small curvature of the phase front,

leads to large errors.

In this section we will show that the well-known Raman-Nath theory can be used to determine the pressure at the focus if an "effective" interaction length replaces the conventional interaction length. The results obtained from the different diffraction orders are consistent and in a good agreement with those calculated by using either Debye's theory or the KZK equation.

DETERMINATION OF PRESSURE AMPLITUDE BY THE LIGHT DIFFRACTION METHOD

The theory of acoustooptic interaction was first developed by Raman and Nath more than half a century ago (Raman and Nath, 1935). The Raman-Nath theory starts from the assumption that the light passing through the ultrasonic beam is only affected in phase, without changing its amplitude or trajectory. This assumption is equivalent to solving Maxwell's equations neglecting the term containing the gradient of refractive index. Raman-Nath theory is also known as the phase grating theory which is associated with the so-called Raman-Nath parameter, v ,

$$v = 2\pi\mu x / \lambda \quad (3.1)$$

v depends on the width of the acoustic beam x , and the ultrasonic pressure. The pressure is proportional to the values of μ , where μ is the refractive index variation and λ is the wavelength of light. Raman-Nath theory is valid for

the case when the Raman-Nath parameter v is very small. Another theory was developed by Biquard and Lucas (1932). In contrast to Raman-Nath theory, this theory starts from the assumption that changes in the light amplitude and its trajectory are important and that the change in phase can be neglected. This so-called Lucas-Biquard theory is valid for larger values of v . More general and more accurate theories were developed later by Wagner (1973), Leroy and Claeys (1984), Hargrove (1962), Klein and Cook (1967), Abeelee and Leroy (1990).

Revised Raman-Nath Theory

Under the assumption that the index of refraction, μ , in the presence of the ultrasonic field of frequency ω^* can be expressed as

$$\mu = \mu_0 + \mu_1 \sin(\omega^* t), \quad (3.2)$$

light diffraction by progressive harmonic waves is well described by the system of difference-differential equations of the generalized Raman-Nath theory. The solution represents the normalized amplitude of the electric field E_n of the n th diffraction order:

$$2 \frac{dE_n}{dv} - E_{n-1} + E_{n+1} = i n^2 Q E_n, \quad (3.3)$$

where v is defined by Equation (3.1), and Q is given by

$$Q = \frac{\lambda^2}{\mu_0 \mu_1 \lambda^{*2}} \quad (3.4)$$

where μ_0 is the refractive index of the undisturbed liquid, μ_1 is the maximum variation of the refractive index due to the ultrasonic wave of wavelength λ^* , and λ is the wavelength of light. In the Raman-Nath approximation, the intensity of the n th-order diffraction peak can be shown to be proportional to the square of the n th-order Bessel function (Cook et al. 1960, 1965, Zankel and Hiedemann 1959, Hargrove 1961, 1968a, 1968b):

$$I_n \propto J_n^2(v) \quad (3.5)$$

v is the Raman-Nath parameter, which can be expressed as

$$v = \frac{2\pi l}{\lambda} \left(\frac{\partial \mu}{\partial P} \right)_s P, \quad (3.6)$$

where P is the acoustic pressure amplitude and the derivative is taken at constant entropy. The parameter l is the light-sound interaction length. The solution given by Equation (3.3) is subject to the limitation that v and Q are both small:

$$v \leq 6, \quad (3.7)$$

$$Q \ll 1 \quad (3.8)$$

When, besides the fundamental frequency, higher harmonics are present, one can express the index of refraction in the ultrasonic field as

$$\mu = \mu_0 + \sum_{j=1}^{\infty} a_j \mu_1 \sin[j(\omega^* t - k^* r) + \phi_j] \quad (3.9)$$

where a_j is the ratio of the amplitude of the j th harmonic to the fundamental, k^* is the acoustic wave number of the j th harmonic, and ϕ_j is the phase factor of the j th harmonic relative to the fundamental. If one considers only the fundamental and second harmonic, the corresponding intensity of diffracted light can be written as (Zenkel and Hiedemann, 1959, Kashkooli et. al. 1987)

$$I_n(v) = \left| \sum_{k=-\infty}^{\infty} J_{n-2k}(v) J_k(a_2 v) \right|^2 \quad (3.10)$$

The intensities of the diffracted light of zeroth, negative and positive first order, i.e. $n=0, -1, 1$, for different ratios of the second harmonic to the fundamental are plotted as shown in Figure 7. One can see that for the higher ratios, the difference between the negative and positive first order diffracted light becomes more obvious. Thus, from the measurement of the asymmetric characteristics of the first order diffracted light intensities, one can obtain the information of the nonlinearity which is a characteristic parameter of the liquid (Kashikoli et. al., 1987), as well as the content of the second harmonic. In the original Raman-Nath formulation, l is simply the depth of the sound beam. The acoustic pressure amplitude along the light path is assumed to be a step function. When the amplitude of the

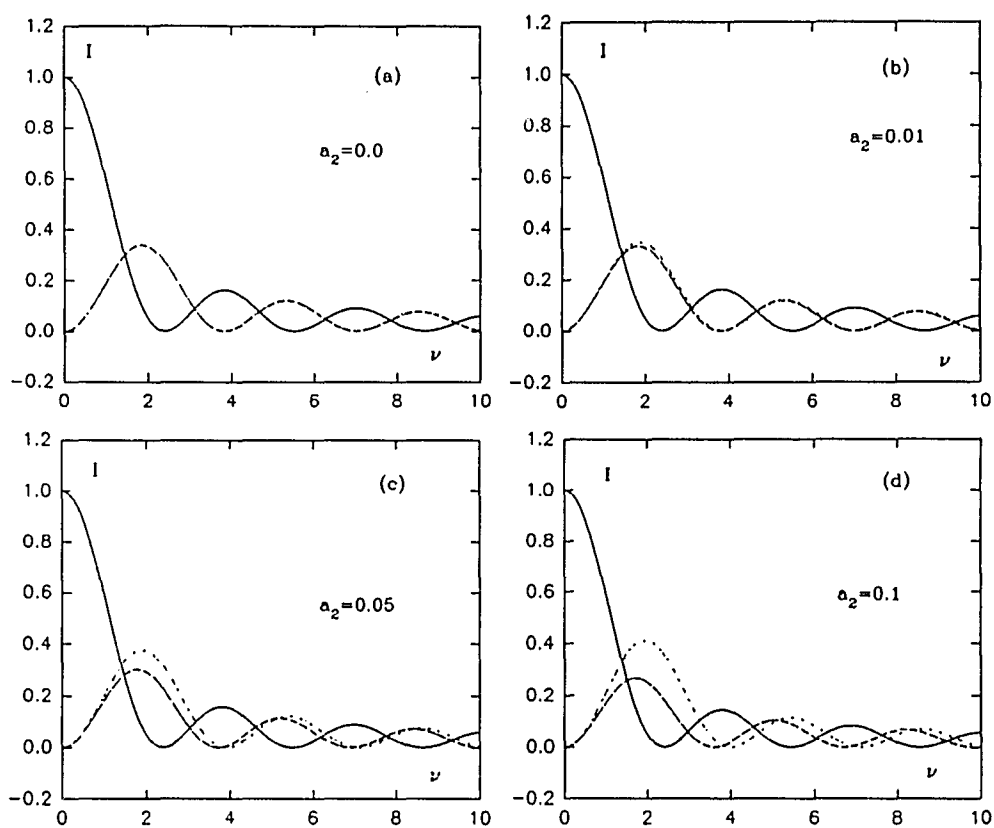


Figure 7. The diffraction light intensities of 0, 1st, -1st orders for different values of $a_2 = 0, 0.01, 0.05, 0.1$.

in a profiled beam, the above assumption is no longer valid. In this case, one can postulate an "effective interaction length" which describes the average effect of the changing pressure distribution along the optical path. We take the spatial average of the pressure distribution along the optical path as the new effective interaction length l^* , which can be written as

$$l^* = \frac{1}{P_m} \int_{-\infty}^{\infty} P(x) dx, \quad (3.11)$$

where P_m is the maximum pressure amplitude. Note that for a material with index of refraction proportional to the acoustic pressure amplitude, $\int P(x) dx$ is proportional to the change in optical path length caused by the pressure of the sound field.

Calculation of Pressure at the Focus from Debye's Theory

In the prefocal region of a converging acoustic wave, the initially spherical wave front gradually flattens out, then passes through the focus, and becomes a diverging spherical wave. The curvature of the wave front experiences a change of sign. Based on the assumption that the radius of wave-front curvature changes continuously and the focus has a finite size, one has the argument that, in the focal region, the focusing spherical wave can be treated as a planar wave with nonuniform amplitude. Its radial distribution in the focal plane can be written, from Debye's theory (P. Debye, 1909,

O'Neil, 1949, Levin et al., 1987)

$$P(r, t) = P_f e^{i[\omega \cdot t + \delta(r)]} \int_0^{\alpha_m} J_0(k^* r \sin \alpha) \sin \alpha d\alpha \quad (3.12)$$

with the condition

$$F \gg \lambda^* \quad (3.13)$$

and with

$$P_f = G P_0 = F k^* (1 - \cos \alpha_m) P_0 \quad (3.14)$$

P_f is the peak pressure amplitude in the focal plane, α_m is the half aperture angle, F is the focal length of the transducer, $J_0(x)$ is the zeroth-order Bessel function, and $\delta(r)$ is a phase factor. P_0 is the pressure on the surface of the transducer, and G is the gain of the transducer.

For $\alpha_m \leq \pi/6$, $\sin \alpha \approx \alpha$ and the time-independent pressure distribution can be approximated as

$$P(r) = P_f \frac{2J_1(kr\alpha_m)}{kr\alpha_m} \quad (3.15)$$

Thus the effective interaction length Equation (3.11) can be expressed as

$$l^* = \frac{2}{P_f} \int_0^{\infty} P(r) dr, \quad (3.16)$$

Upon substituting Equation (3.15) into (3.16), we get

$$l^* = 4 \int_0^{\infty} \frac{J_1(k^* \alpha_m r) dr}{k^* r \alpha_m}, \quad (3.17)$$

which gives

$$l^* = \frac{4}{k^* \alpha_m} \quad (3.18)$$

Here we have ignored the phase factor $\delta(r)$ in Equation (3.12), and we will show later that it has negligible influence on the final result.

If $\alpha_m > \pi/6$, then the integral can be solved by series expansion. The special case of $\alpha_m = \pi/2$ is of considerable practical importance and is easily written as a recursion relation

$$P(r) = P_f \sum_{j=0}^{\infty} A_j \quad (3.19)$$

$$A_0 = 1 \quad (3.20)$$

$$A_j = - \left[\frac{kr}{2} \right]^2 \frac{2}{j(2j+1)} A_{j-1}. \quad (3.21)$$

The zeroes of this function occur when $kr = m\pi$ where $m=1,2,3,\dots$. Substituting Equation (3.19) into Equation (3.16), one can get

$$l^* = 2r \sum_{j=0}^{\infty} B_j \quad (3.22)$$

$$B_0 = 1 \quad (3.23)$$

$$B_j = - \frac{2(2j-1)}{j(2j+1)^2} \left[\frac{kr}{2} \right]^2 B_{j-1} \quad (3.24)$$

In the limit as r goes to infinity, l^* approaches $\lambda^*/2$

where λ^* is the acoustic wavelength.

Substituting Equation (3.18) or (3.22) into (3.6), one can relate the Raman-Nath parameter v to the pressure amplitude P_f , for small and large aperture angle respectively. For the transducer with small aperture angle, one can get

$$v = \frac{4\lambda^*}{\alpha_m \lambda} \left(\frac{\partial \mu}{\partial P} \right)_s P_f \quad (3.25)$$

The Pressure Distribution Calculated from the KZK Equation

So far, we have neglected nonlinearity and dissipation of the liquids. Directive acoustic beam in which the effects of nonlinearity, diffraction, and dissipation are important may be modeled by using the KZK equation which provides an accurate model of directive finite amplitude sound beams in dissipative fluids. The KZK equation may be written in the dimensionless form, given by Hart and Hamilton (1988)

$$\frac{\partial^2 P'}{\partial \tau \partial \sigma} - \frac{1}{4} \nabla^2_{\perp} P' - A \frac{\partial^3 P'}{\partial \tau^3} = \frac{B}{2} \frac{\partial^2 P'^2}{\partial \tau^2}, \quad (3.26)$$

$$\sigma = \frac{Z}{F}, \quad (3.27)$$

$$A = \sigma F, \quad (3.28)$$

$$B = \frac{\beta \omega^* P_0 F}{\rho_0 C_0^3}, \quad (3.29)$$

where P_0 is the acoustic pressure field amplitude on the

$$\tau = \omega^* \left(t - \frac{z}{c_0} \right), \quad (3.30)$$

$$P' = \frac{P}{P_0}, \quad (3.31)$$

surface of the transducer and c_0 is the speed of sound in the medium. The z axis is taken along the propagation direction of the acoustic beam. The parameter α accounts for thermal and viscous losses, β is the coefficient of nonlinearity, and ρ_0 is the density of the liquid. The transverse Laplacian operator ∇_{\perp}^2 accounts for wave-front curvature associated with diffraction. The focal plane is defined to be at $\sigma = -1$ and radiating in the $+\sigma$ direction. The terms in Equation (3.26) are defined as follows.

σ is the reduced axial coordinate.

τ is the dimensionless retarded time.

$\omega = 2\pi f$ is the source angular frequency.

∇_{\perp}^2 operates on the reduced transverse coordinate $\vec{s} = \sqrt{G} \frac{\vec{r}}{F}$.

$\nabla_{\perp}^2 = \frac{\partial^2}{\partial s^2} + \frac{1}{s} \frac{\partial}{\partial s}$ for an axisymmetric field, where $s = |\vec{s}|$.

The system is governed by three parameters A , B , G .

A is the linear absorption coefficient (in nepers) at the focal plane.

B is a dimensionless source amplitude accounting for the nonlinearity of the liquid.

$G = z_0/F$ is the linear focusing gain of the system,

where $z_0 = \omega F^2 / 2c_0$ is the Rayleigh distance. In the absence of both absorption ($A=0$) and nonlinearity ($B=0$), the solution

for radiation from a focused transducer yields a dimensionless pressure amplitude $|P|$ equal to G at the geometric focus.

The lossless form of Equation (3.26) (i.e. with $A=0$) was derived by Khokhlov and Zabolotskaya (1969), whose result was subsequently extended by Kuznetsov (1971) to include thermoviscous losses. Later, Naze Tjøtta and Tjøtta (1981) rederived Equation (3.26) by requiring that the nonlinearity, diffraction and absorption be accounted for to the same order of magnitude. Additionally, Equation (3.26) is derived under the assumption that the acoustic beam is well collimated (i.e. $kF \gg 1$).

The numerical method to solve Equation (3.26) has been studied by Hart (1987). To increase the efficiency of the numerical solution, a coordinate transformation needs to be introduced that follows the convergent geometry of a focused ultrasonic beam. A Fourier series expansion of the acoustic pressure is used to reduce the transformed KZK equation to a set of coupled parabolic equations. He used the implicit backward finite difference method to obtain the numerical solutions. He also derived the approximate analytic solution to Equation (3.26) and compared it with the results from the numerical method. The transformation that is introduced by Hart and Hamilton (1988) can be written as

$$T(u, \sigma, \theta) = (\sigma \pm \delta) P(s, \sigma, \tau) \quad (3.32)$$

where δ is a small positive quantity that governs the rate at which the transformed geometry converges. With $\delta \ll 1$, length

$$\vec{u} = \frac{\vec{S}}{\sigma \pm \delta} \quad (3.33)$$

$$\theta = \tau - \left(\frac{S^2}{\sigma \pm \delta} \right) \quad (3.34)$$

scales in the focal plane are δ times smaller than at the source. Note that the transformed coordinates are singular in the focal plane when $\sigma=0$. The minus signs in Equations (3.32)-(3.34) are used in the prefocal region ($\sigma < 0$), and the plus signs beyond the focus ($\sigma > 0$). Substitution of Equations (3.32)-(3.34) into Equation (3.26) yields

$$\left[\frac{\partial^2}{\partial \tau \partial \theta} - \frac{1}{4(\sigma \pm \delta)^2} \nabla_u^2 - A \frac{\partial^3}{\partial \theta^3} \right] T = \frac{B}{2(\sigma \pm \delta)} \frac{\partial^2 T^2}{\partial \theta^2} \quad (3.35)$$

With the transformed pressure amplitude T expanded in a Fourier series

$$T(\vec{u}, \sigma, \theta) = \sum_{n=1}^{\infty} t_n(u, \sigma) \sin[n\theta + \psi_n(u, \sigma)] \quad (3.36)$$

$$= \sum_{n=1}^{\infty} g_n(u, \sigma) \sin(n\theta) + h_n(u, \sigma) \cos(n\theta)$$

where

$$g_n = t_n \cos(\psi_n) \quad (3.37)$$

$$h_n = t_n \sin(\psi_n) \quad (3.38)$$

Equation (3.35) can be transformed into the set of coupled equations for g_n , h_n .

$$\begin{aligned} \frac{\partial g_n}{\partial \sigma} = & -n^2 g_n + \frac{1}{4n(\sigma \pm \delta)^2} \nabla_u^2 h_n \\ & + \frac{nB}{2(\sigma \pm \delta)} \left[\frac{1}{2} \sum_{k=1}^{n-1} (g_k g_{n-k} - h_k h_{n-k}) - \sum_{p=n+1}^{\infty} (g_{p-n} g_p + h_{p-n} h_p) \right] \end{aligned} \quad (3.39)$$

and

$$\begin{aligned} \frac{\partial h_n}{\partial \sigma} = & -n^2 h_n - \frac{1}{4n(\sigma \pm \delta)^2} \nabla_u^2 g_n \\ & + \frac{nB}{2(\sigma \pm \delta)} \left[\frac{1}{2} \sum_{k=1}^{n-1} (h_k g_{n-k} + g_k h_{n-k}) + \sum_{p=n+1}^{\infty} (h_{p-n} g_p - g_{p-n} h_p) \right]. \end{aligned} \quad (3.40)$$

Suppose the approximate solution consists of N number of harmonics, one can replace the infinite sign in Equation (3.39) and (3.40) with N and use the finite difference method to get the numerical solutions to the Equation (3.26), subject to the boundary conditions.

The solution to Equation (3.26) along with a measurement of P_0 provides the counterpart to the results obtained from light-diffraction theory. One can determine the pressure at the focus as a function of input power by measuring the diffracted light and compare the results with those determined independently by either the theory of Debye or solutions to the KZK equation to test the modified Raman-Nath model.

CALCULATION OF PRESSURE AMPLITUDE IN WATER WITH DIFFERENT APPROACHES

A PZT-4 (Staveley Sensors, East Hartford, CT) spherical concave piezoelectric transducer was suspended in a rectangular container with glass windows on the sides. Both the convex and concave sides of the transducer were silver coated. A three point support on the bottom served as one electrical contact and three springy metal wires provided contact on the top or concave side of the transducer. A Hewlett-Packard 651B oscillator is used to drive the transducer. The electrical signal from the oscillator is amplified by a homemade RF amplifier before being applied to the transducer. There is no impedance matching layer on either concave or convex side of the transducer. The liquid used is distilled water with specific resistance over $10\text{M } \Omega / \text{cm}$; the value of $\left(\frac{\partial \mu}{\partial P}\right)_s$ is equal to $14.66 \cdot 10^{-11} \text{Pa}^{-1}$. α is equal to 1.50 and β is equal to 6.0. The transducer with the series resonance frequency at 2.15MHz, has a radius of curvature of 2.54cm, a thickness of 0.028cm, and an aperture angle of 26.66° . Using the method described in the Appendix, we are able to determine the pressure on the surface of the transducer. Then either Debye's formula or the KZK equation was used to calculate the pressure in the focal plane.

The light from a He-Ne laser with output power of 0.8 mW and beam size of 0.8 mm passes through the windows on the container and through the focal plane of the transducer. The

beam is perpendicular to the propagation direction of the sound beam. The vertical diffraction pattern, parallel to the propagation direction of the acoustic wave, is measured using a photodiode (UDT3DP1). The output of the photodiode was amplified so that the electrical signal corresponding to the undiffracted laser beam was about 8 V. The photodiode was scanned through the beam spot to collect the optical signal, i.e. the diffraction intensities for the first three orders, and the signal was recorded with a X-Y recorder. Figure 8 shows the measured light diffraction intensities for the zeroth, negative and positive first diffraction orders versus the applied voltage. Note that the higher orders of diffraction are observed but not used in our analysis because no additional useful information is provided by these higher orders.

By the method described in the Appendix, we obtained the relationship between the surface pressure amplitude and the applied voltage to the transducer. Thus we have a relation between the surface pressure and the various light intensities. From the light intensities, we calculated (using Equation (3.10)) the Raman-Nath parameter and a_2 . We found that an a_2 of approximately 0.04 best represents our data. Via Equation (3.25) the Raman-Nath parameter gave the peak pressure in the focal plane.

Figures 9, 10, and 11, show the pressure amplitudes obtained from our modified model for the zeroth, negative and

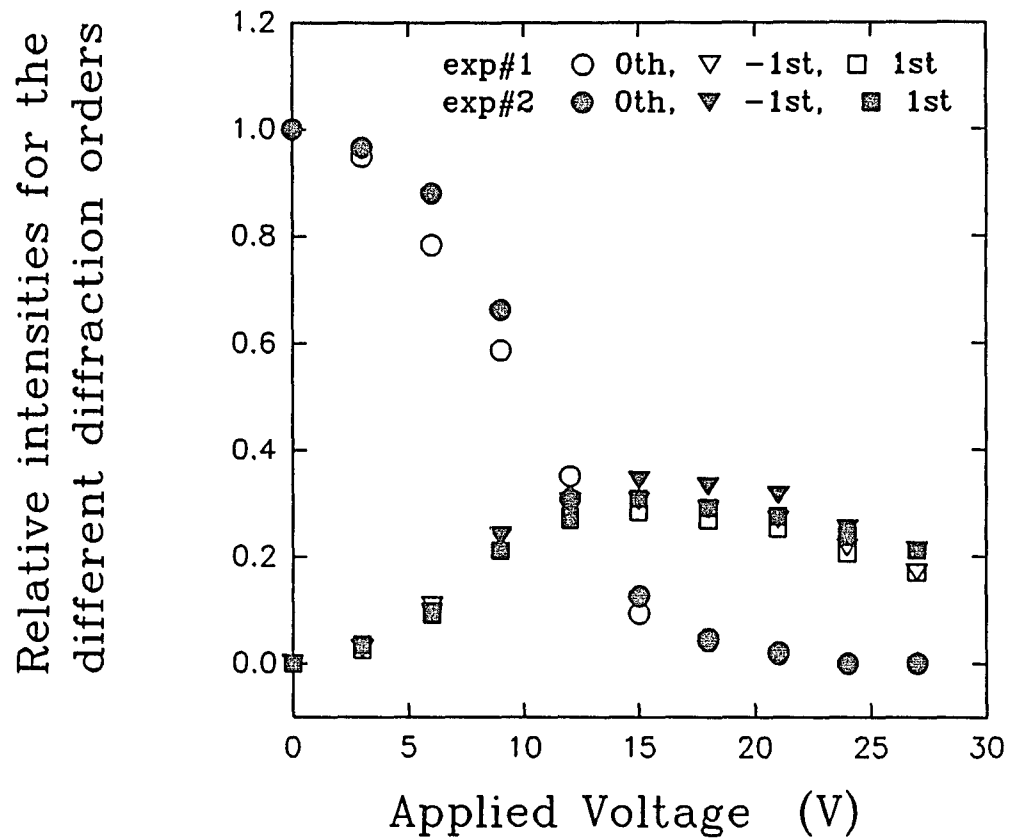


Figure 8. Measured light intensities relative to the intensity of the undiffracted beam for the zeroth, positive, and negative first diffraction orders vs. the applied voltage.

positive first order of the diffracted light. The following can be observed: Agreement between the modified Raman-Nath model (Equations (3.10) and (3.25)) and Debye's theory (Equation (3.14)) and the calculation using the KZK equation is good and results obtained from all the three different diffraction orders are consistent. The peak pressure according to the KZK equation is less than that which is obtained from Debye's theory because the absorption and nonlinearity are being considered. Because the changes in intensity of the diffracted light is smaller for larger amplitudes, the measured pressure amplitudes from the different diffraction orders are more uncertain than those obtained for smaller amplitudes. When the Raman-Nath parameter is around two (a pressure of about 12 atm), the diffraction intensity of the zeroth order is very close to zero but intensities of both the negative and positive first orders are close to maximum. Therefore, the pressure amplitude determined by the diffracted light of the zeroth order is not as accurate as that determined by the positive and negative first orders. Note that in Figs. 9, 10, and 11, we used our effective interaction length to replace the "standard" light-sound interaction length.

Following the method developed by T. Hart, we solved the KZK equation numerically with all of the parameters determined by our system. The acoustic gain coefficient G is 28, the loss coefficient A is 0.0038 and nonlinearity constant B

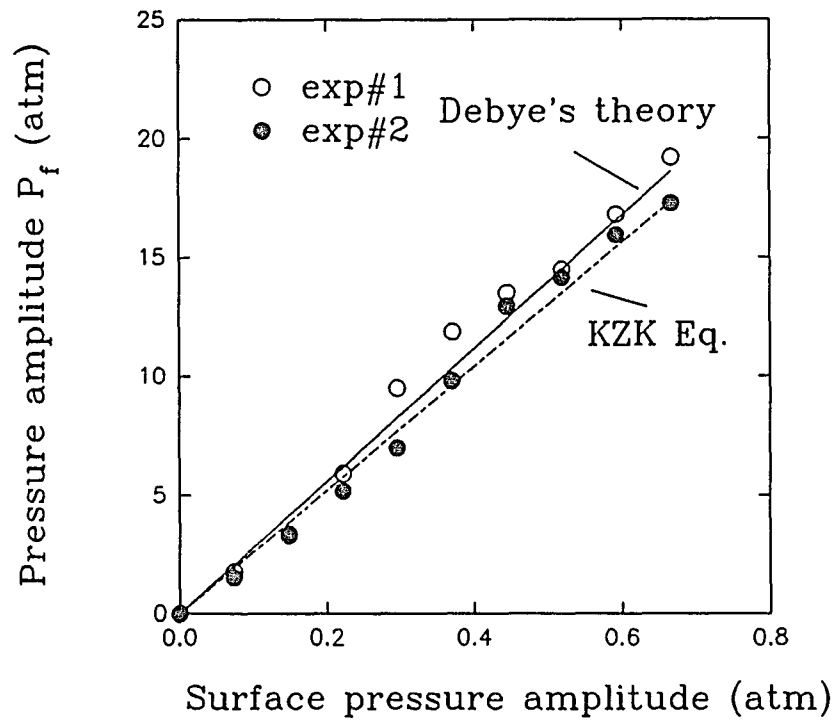


Figure 9. Pressure at the focal point vs. the surface pressure on the transducer calculated from zeroth-order diffraction, and comparison with the results from Debye's theory and the KZK equation.

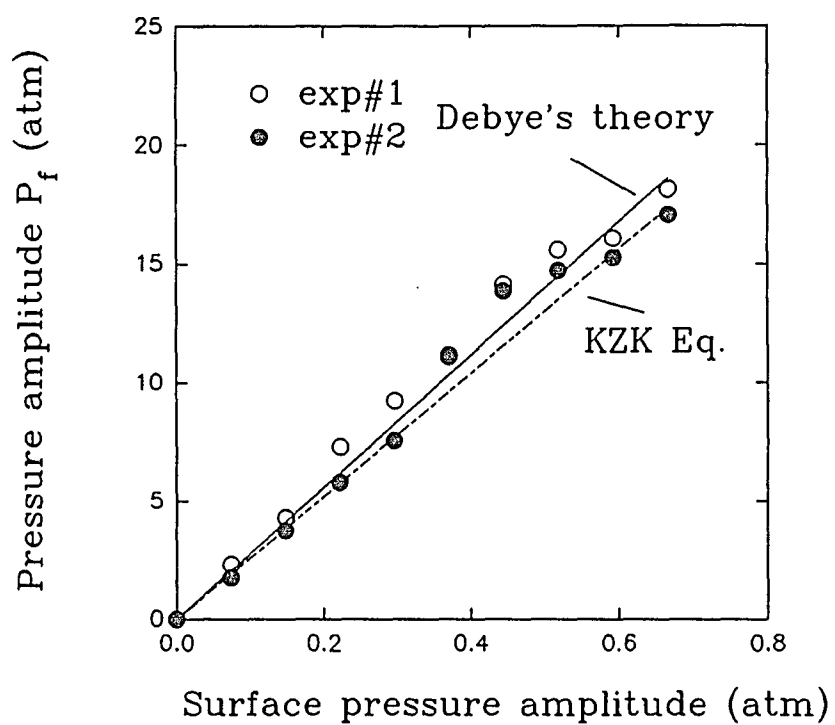


Figure 10. Pressure at the focal point vs. the surface pressure on the transducer calculated from the diffraction order of +1, and comparison with the results from Debye's theory and the KZK equation.

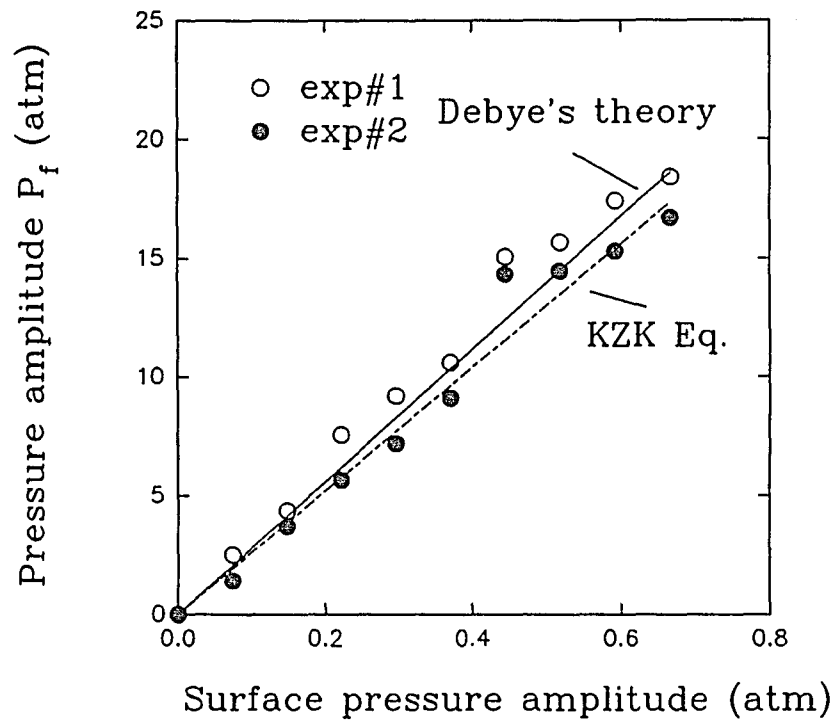


Figure 11. Pressure at the focal point vs. the surface pressure on the transducer calculated from the diffraction order of -1, and comparison with the results from Debye's theory and the KZK equation.

is in the range from 0 to 0.025 corresponding to a pressure at the source of up to about 1 atmosphere. In order to determine the proper value of the parameter δ which controls the convergence of the program, we calculated the normalized pressure distribution along the propagation direction and found that δ should be equal to 4.5. With this value for δ , we performed calculations of the axial and radial pressure distributions by including the first four harmonics. The calculated axial pressure distribution (along the propagation direction) is shown in Figure 12(a), (b), (c), (d) for different values of parameter B. The transverse distribution (in the focal plane) is shown in Figure 13(a), (b), (c), (d). For low pressures, only the fundamental harmonic is important. In this case, Debye theory obtains (Equation (3.14)). For the higher pressures, higher harmonics show up as shown in Figures 12 and 13.

The solution to the KZK equation with the material constants of water and the pressure amplitude at the surface of the transducer as the only input data, gives us an approximate way to calculate a_2 , the amount of second harmonic. From Figure 13(b), the ratio of the pressure amplitude of the second harmonic to that of the fundamental is found to be 0.065. This is not equal to a_2 , however since the region where the second harmonic is important is smaller than the region in which the fundamental contributes to the light scattering; the second harmonic is focused to a smaller spot.

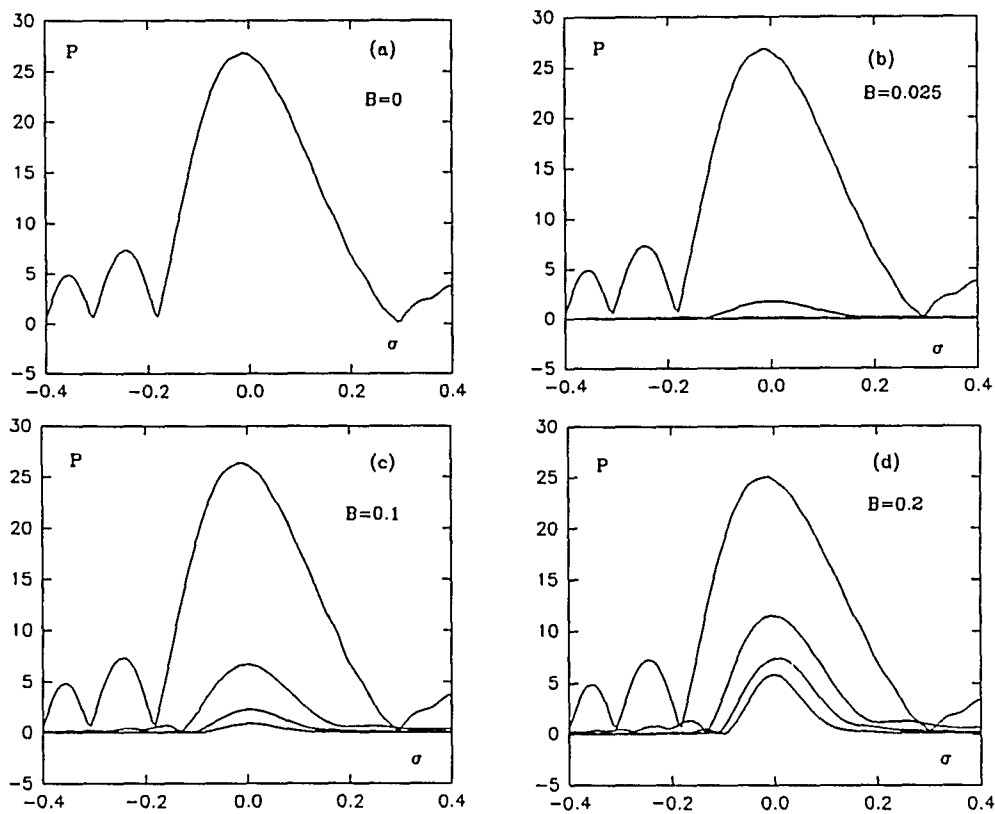


Figure 12. The axial pressure distributions calculated from the KZK equation with values of 0, 0.025, 0.1, 0.2, for the nonlinearity parameter B .

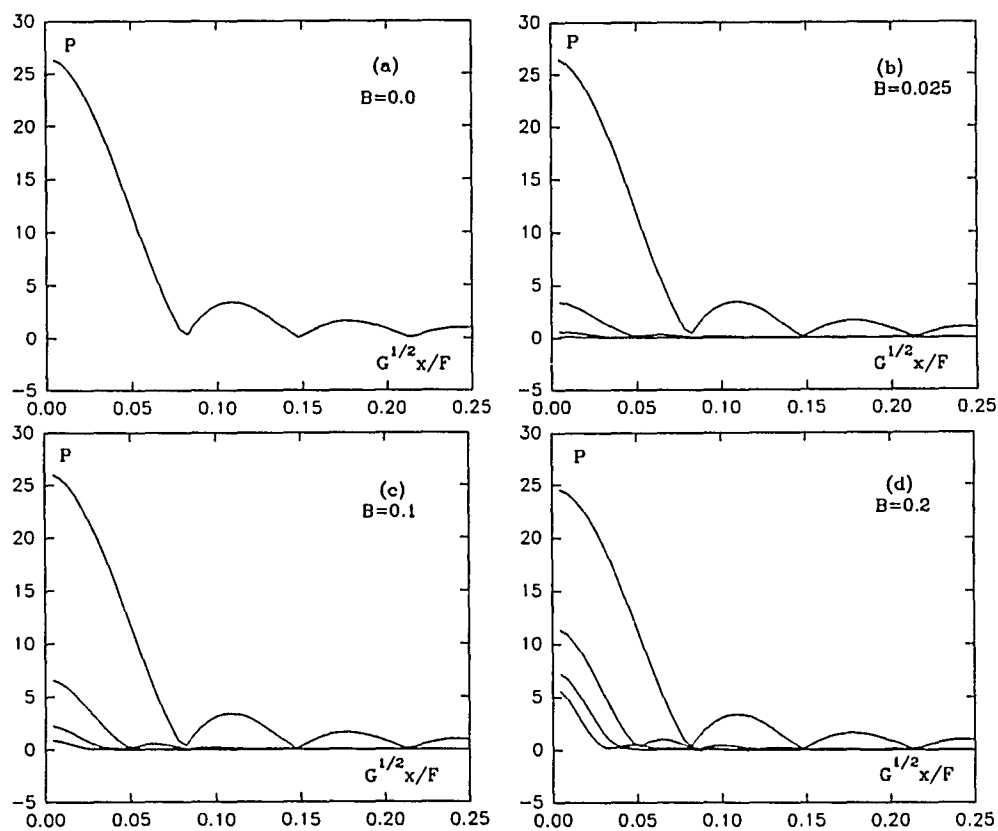


Figure 13. The transverse pressure distributions in the focal plane calculated from the KZK equation with values of 0, 0.025, 0.1, 0.2, for the nonlinearity parameter B .

In order to calculate the effective a_2 , one has to perform the integration of Equation (3.11) with $P(x)$ being the pressure distribution of the second harmonic. An approximate value can be obtained by comparing the width at half maximum of the central peak for the second harmonic pressure distribution with the corresponding width of the fundamental. Doing this gives an effective a_2 of 0.04. This is in good agreement with our observation of the asymmetry in the light diffraction patterns (Zankel et al., 1959).

By solving the KZK equation, we also obtain the phase factors $\delta_j(r)$. To assess the approximate influence of these phase factors, one can compare $P_j(r)\cos(\delta_j(r))$ with P . When the integration in Equation (3.16) is performed, one can argue that only the real part plays a role. Calculations show that the difference between $P_j(r)$ and $P_j(r)\cos\delta_j(r)$ is negligible and thus we can ignore the phase factors. Therefore the effective interaction length calculated with the numerical results from the KZK equation is not very different from that obtained from the Debye's theory in the pressure range that we are concerned with.

CHAPTER IV

MEASUREMENT OF THE TENSILE STRENGTH OF LIQUID NITROGEN

Up to this point, all of the necessary theoretical procedures required to proceed with the measurement of the tensile strength of liquid nitrogen have been described. As mentioned in Chapter II, the well-known formula from the classical nucleation theory, Equation (2.22) is to be tested experimentally. This work is based on the fact that in the region of positive pressure, Equation (2.22) has been shown to be valid for liquid nitrogen from the results of the superheating experiment (Sinha et al., 1987). Sinha et al. studied homogeneous nucleation in liquid nitrogen in the temperature range from 77.4 K to 124.6 K and this corresponds to the pressure range $0.03 < P_v/P_c < 0.91$, where P_v and P_c are the saturated vapor pressure and the critical pressure of the liquid. It is believed that the T-P curve obtained from Equation (2.22) can be continuously extended into the negative pressure region. Based on this basic assumption, the experimental results can be compared with those obtained from Equation (2.22) for different nucleation rates. From the analysis of the different techniques of measuring the pressure in a liquid in Chapter III, any of the mentioned methods (i.e., the light diffraction, the Debye's theory and solving

the KZK equation) can be used to determine the tensile strength of liquid nitrogen. Because both Debye's theory and the KZK equation are similar (the surface pressure at the transducer has to be known), the measurement of the tensile strength is really carried out using only two independent methods, the light diffraction and the Debye's theory.

The principal advantage of using focused ultrasonic wave to induce the homogeneous nucleation in the liquid nitrogen is as follows. Since a short ultrasonic pulse is focused onto a very small volume of the bulk liquid, the possibility of heterogeneous nucleation caused by the impurities or walls can be greatly reduced. We adopt the method developed by Nissen (1988, 1989) to obtain the measurement of the tensile strength of liquid nitrogen. Although he used a hemispherical transducer, we will use ultrasonic transducers with a small aperture angle since the theories concerning this kind of transducer are well developed. In this chapter, we will describe our experimental procedures in some detail and present our experimental results.

THE DESIGN OF THE HIGH PRESSURE DEWAR

To measure the tensile strength of liquid nitrogen, a dewar that is able to withstand high pressure is needed. It requires windows in the walls on both sides so that the laser beam can pass through. A stainless steel Dewar with windows in the walls as shown in Figure 14 was designed by our

laboratory and manufactured by the machine shop. The inner and outer diameters of the Dewar are 3" and 8.25" respectively, and it is 42" long. The inner windows with the thickness of 1.0 cm are sealed with indium O-rings. The outer windows having a thickness of 1.0 cm and also the top are sealed with rubber vacuum O rings. The vacuum in the space between outer and inner wall is achieved using two mechanical pumps working concurrently. The maximum vacuum level obtained is less than $10 \mu\text{ m}$ at room temperature and $5 \mu\text{ m}$ when cooling down. The accessible pressure range of the Dewar is from 1 to 10 atm. There are three liquid level sensors inside the Dewar to test the surface of liquid nitrogen in order to monitor the amount of liquid nitrogen in the dewar. A temperature indicator (Tektronics Model P6601) is located above the transducer near the region of interest to monitor the temperature during the measurement and to make sure that the measurements are taken in the equilibrium state on the coexistence curve. The temperature measurement is accomplished through the use of a thin-film platinum resistor located at the tip of the Tektronics probe. The temperature coefficient of resistance of the platinum resistor is the parameter used to determine temperature. Resistance may be expressed as a function of temperature:

$$R(T) = R_0 + \alpha T + \delta T^2, \quad R_0 = 100 \Omega, \quad \alpha = 0.3738 \Omega/^{\circ}\text{C}, \quad \delta = -8.85 \cdot 10^{-5} \Omega/^{\circ}\text{C}^2,$$

T is measured in degrees C.

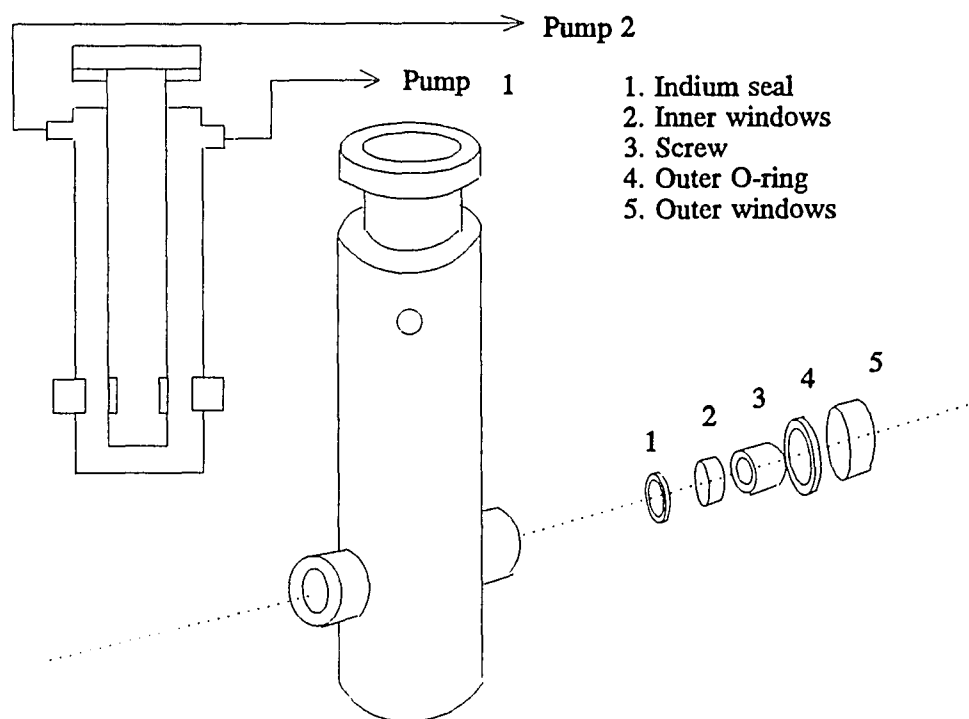


Figure 14. The stainless steel dewar built for measurement of the tensile strength of liquid nitrogen.

EXPERIMENTAL SETUP AND MEASUREMENT OF THE PARAMETERS OF THE TRANSDUCER

The experimental setup can be described by Figure 15. There are three oscilloscopes being used in the experiment, with A (Tektronics TM515), and B (Tektronics 2221A) used to monitor the voltage signal before and after amplification. If the voltage after the amplification is high then an attenuator is needed. C (Tektronics 2201) is for displaying the optical signal of the zeroth order diffracted light which is collected by a photodetector and amplified by a home-made amplifier. The optical signal can be transferred to a PC to be stored and analyzed or downloaded to a printer directly. Figure 16 shows schematically how the laser beam is scattered by the focused ultrasonic wave and the optical signal collected.

A PZT4 spherical transducer with diameter of 1" and an aperture angle of 26.6 degree, with a resonant frequency of 2.15 MHz was used first. To determine the characteristic parameters (resistance, inductance and capacitances) of the transducer, a gate circuit was implemented. The input and output voltages as a function of frequency were measured. The characteristic parameters were obtained through fitting the experimental data with the equivalent electrical circuit model using the method as shown in the appendix.

The parameters in both air and liquid nitrogen were determined in order to separate the load due to dissipation of acoustic field varies greatly along the optical path such as

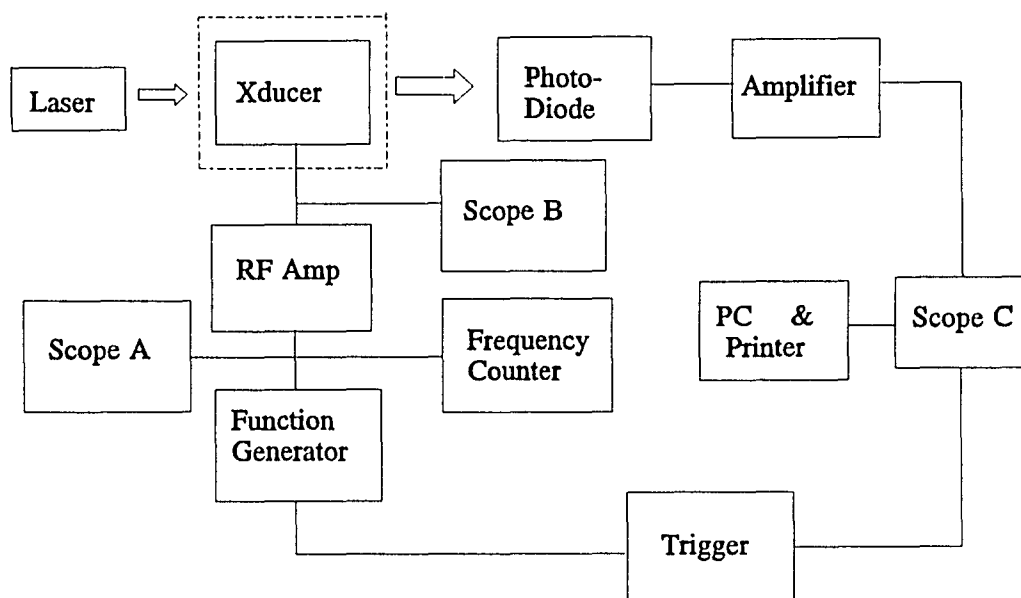


Figure 15. The diagram of the experimental setup for measuring the tensile strength of liquid nitrogen.

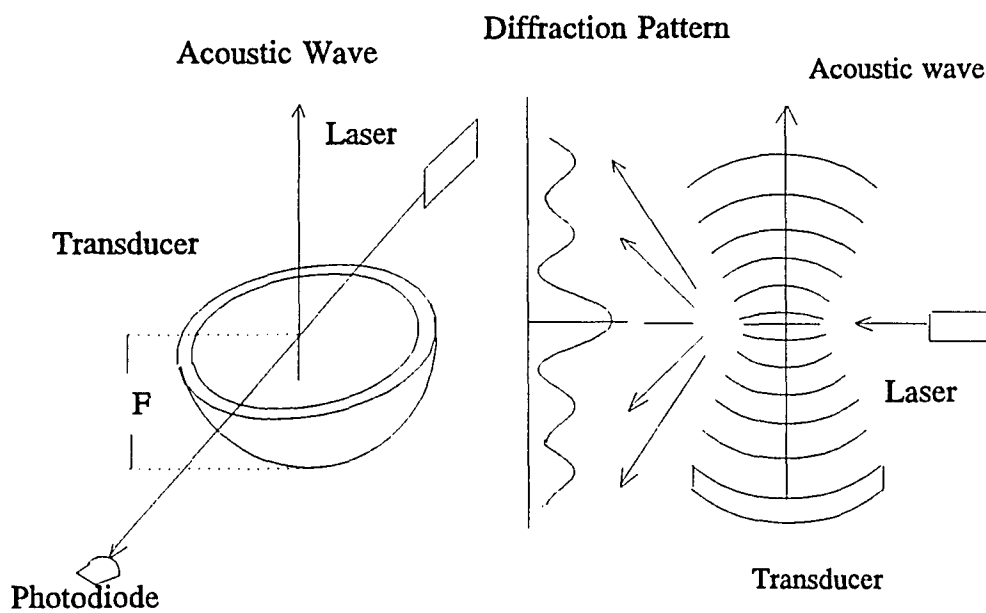


Figure 16. Schematic diagram of the light diffraction by a focused ultrasonic wave. F is the focal length of the transducer.

energy into the liquid nitrogen and into the supports of the transducer. The parameters found are

In air,

$$R=30\Omega , L=3.0\cdot 10^{-4}H , C_0=0.2pF , C=18.6pF .$$

In liquid nitrogen,

$$R=87\Omega , L=0.22mH , C_0=0.2pF , C=24.8pF .$$

We also measured the characteristic parameters of a transducer with the same geometric parameters but with a different resonance frequency of 1 MHz.

In air,

$$R=7\Omega , L=3.15mH , C_0=2pF , C=1.24pF .$$

In liquid nitrogen,

$$R=34\Omega , L=2mH , C_0=2pF , C=1pF .$$

MEASUREMENT

Experimental Procedures

The alignment of the optical path and the determination of the focal region of the transducer. Because the windows are very small the transducer cannot be seen from the window, it is necessary to be certain that the position indicator is visible from the windows on the wall of the dewar so that the focal point of the transducer can be located. After enough liquid nitrogen is transferred into the Dewar, an oscillator is connected to the transducer directly. A voltage of about 30 volts is applied to the transducer. An image of the laser

beam which passed through the windows was observed on a screen. Carefully adjusting the beam, one can obtain the diffraction pattern easily. If the light beam passes through the focal point of the acoustic transducer, the maximum number of diffraction fringes can be obtained. The photodetector is then aligned with the laser beam and a lens of focal length 15cm placed in between the photo-diode and the window of the dewar. By carefully adjusting the position of the photodiode, a maximum optical signal can be obtained and observed by the oscilloscope.

The Measurement of the Tensile Strength of Liquid Nitrogen. Once the resonance frequency of the transducer and the focal point of the acoustic field are determined, one can start to measure the tensile strength of liquid nitrogen. In this case, the oscillator used in the process of locating the focal point was replaced by a function generator. A pulse generator provides the gate signal to the function generator as well as the trigger signal to the oscilloscopes. The pulse width is chosen in the range of 0.2-2 msec. The pulse shape is demonstrated in Figure 17. A necessary step to take before measuring the tensile strength of liquid nitrogen is to double check to make sure that it is at an equilibrium state on the coexistence curve. To do so, the measurements of temperature in the liquid nitrogen and the vapor pressure are taken and the vapor pressure is controlled by opening or closing the valve on the Dewar. One can start out with highly repetitive

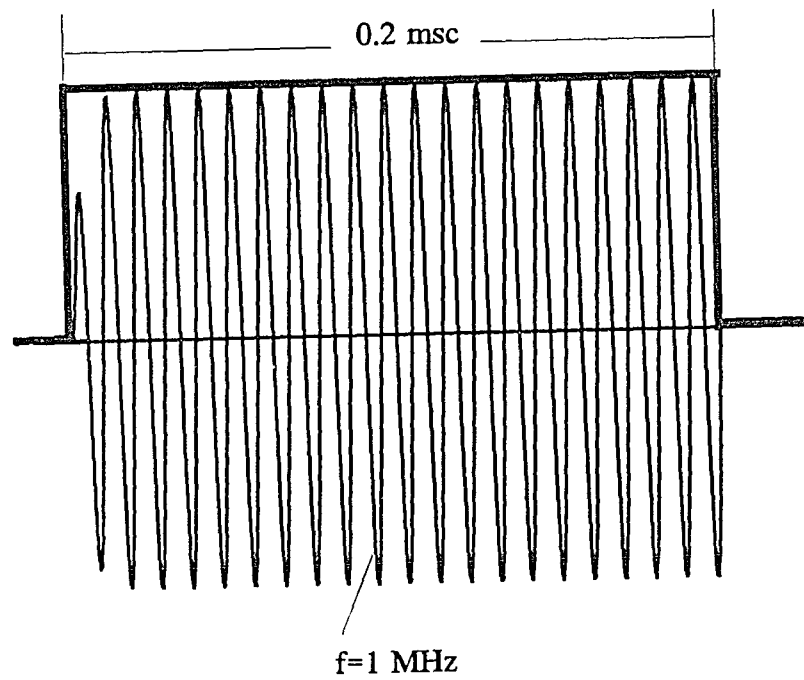


Figure 17. Schematic diagram of the electrical pulse applied to the transducer of 1 MHz.

pulse excitation to estimate the approximate range within which homogenous nucleation occurs. Next a single pulse mode is chosen in order to measure the tensile strength of liquid nitrogen more precisely. The measurement of the tensile strength of liquid nitrogen was first performed under a condition of atmospheric pressure for the vapor phase in the dewar. If the voltage on the transducer is zero, i.e. no ultrasonic field present, the measured signal of incident light is at its highest level. It then takes about $28.5 \mu\text{s}$ for the acoustic wave to reach the focal point and start to interact with the incident laser beam. This time period can be calculated from the speed of sound in liquid nitrogen and the focal length. As the voltage applied to the transducer increases, there is a time delay as the acoustic energy builds up at the focus, i.e. the pressure amplitude increases to a maximum and consequently the intensity decreases to a lower level. The measured intensity of the zeroth order (transmitted) light decreases continuously with an increase of voltage on the transducer. There exists a critical point where one can observe that the intensity of the zeroth diffraction light drops below a certain lower level then suddenly starts to fluctuate because homogeneous nucleation occurs. The corresponding pressure at the focus is taken as the tensile strength of the liquid nitrogen. At atmospheric pressure, it reaches the critical point when the voltage on the transducer is about 130V. The signal representing the

intensity of the zeroth diffraction light drops from its highest level of about 14 V to about 3 V and the pressure amplitude at this moment is calculated to be about -91 atm. If the vapor pressure in the dewar increases, the tensile strength of the liquid nitrogen decreases (see Figure 5) and so does the corresponding critical voltage on the transducer. Figure 18 shows the transmitted light intensities recorded by the oscilloscope for a 2 MHz transducer at a voltage less than necessary for reaching homogeneous nucleation and a voltage just sufficient to homogeneously nucleate the liquid. Figure 18 shows transmitted light intensities for a 1 MHz transducer on different time scales when homogeneous nucleation is observed. In Figure 18 (a), the lower trace is the trigger pulse which controls the pulse width of the electrical signal on the transducer. Figure 19 is for a 1 MHz hemispherical transducer before and when homogeneous nucleation is reached.

Several observations can be made from Figures 18 through 20. Below the critical voltage, the laser beam is partially scattered out of its propagation direction and the intensity of the transmitted light drops to a lower level but remains stable in time. When the critical voltage is reached, the liquid nitrogen at the focal region is stretched out of the limit of its stable structure and homogeneous nucleation occurs. Subsequently, the growing bubbles leave the focal region while more bubbles are generated. If the number of bubbles in the focal region and their size is large enough the

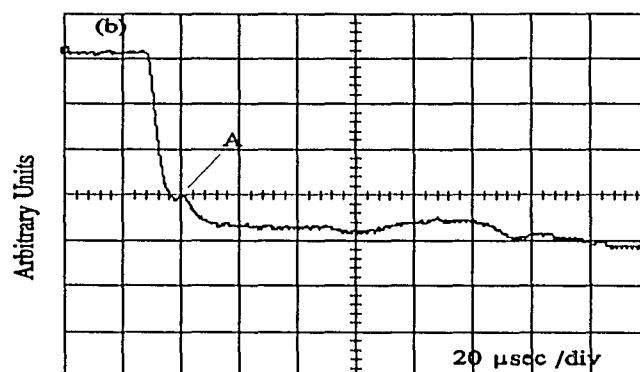
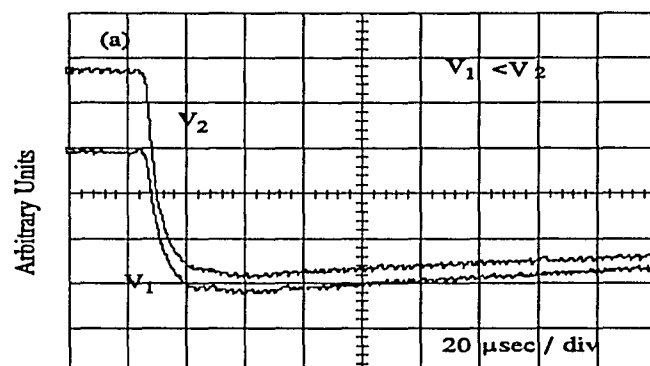


Figure 18. Transmitted light intensity for different voltages on the transducer of 2 MHz. (a) when homogeneous nucleation is not reached and (b) when homogeneous nucleation is reached.

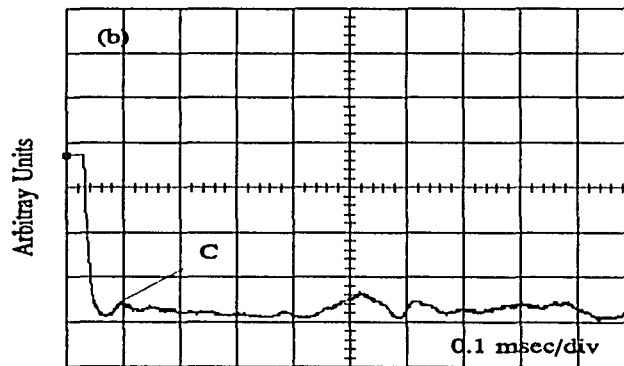
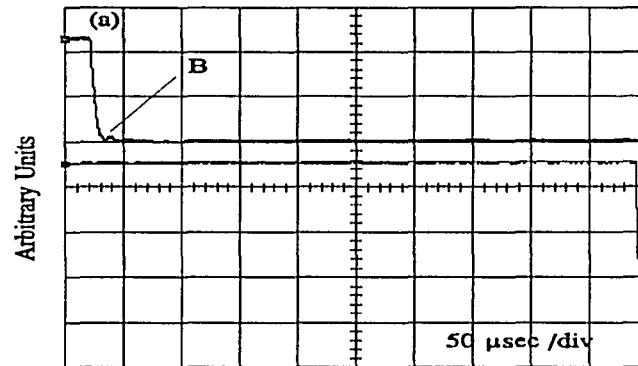


Figure 19. Transmitted light intensity for 1 MHz transducer with small aperture angle on different time scales. (a) 50 μ sec/div. and (b) 0.1 msec/div.

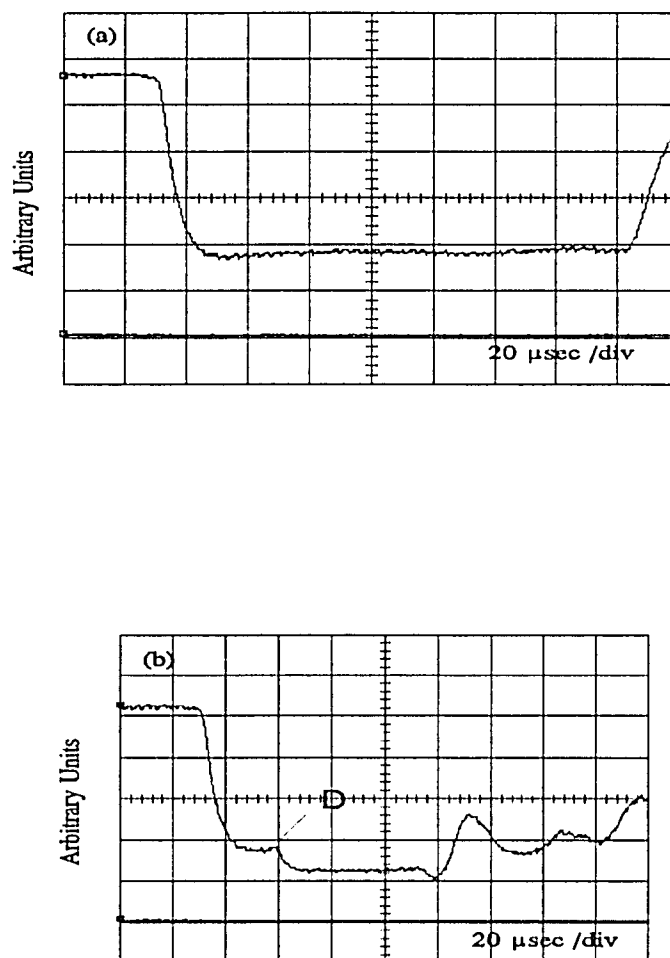


Figure 20. Transmitted light intensities for 1 MHz hemispherical transducer. (a) When homogeneous nucleation is not reached and (b) When the homogeneous nucleation is reached.

light beam through the focal region is affected and the transmitted light intensity starts to fluctuate rapidly. However, the tensile strength of liquid nitrogen should be reached sometime before this violent process can be observed. From Figures 18(b), 19, 20(b), one can see that at certain points (A, B, C, D), the first peak which is believed due to the homogeneous nucleation appears. This kind of signal was also observed by Nissen (1988, 1989) in his study of the tensile strength of liquid helium. He defined the signal as the characteristic signal of the homogeneous nucleation. Although the detailed mechanism that causes this peak is not clear, one possibility seems to be that when the tensile strength of liquid nitrogen is reached, or the liquid is about to break, the liquid becomes softer, the local pressure amplitude at the focal region decreases so that the transmitted light intensity increases. Nissen (1988) explained the appearance of this characteristic signal of the homogeneous nucleation from a different approach. His argument is as follows. Immediately after nucleation begins, the bubbles are too small to scatter the light, but they are absorbing power from the acoustic wave as they grow. The absorption of power manifests itself as decrease in the acoustic pressure amplitude, causing an increase in the transmitted light intensity. When the bubbles have grown large enough to scatter the laser beam, the light intensity decreases again. This assumption cannot explain the flat

region in between the first peak and quick fluctuation occurring later, which we have observed repeatedly in our experiments with liquid nitrogen. Despite the fact that our explanation for the peak is different we still associate the tensile strength of the liquid with it.

The characteristic signal is associated with the homogeneous nucleation also because a sudden jump of the electrical signal at the transducer occurs about $28 \mu\text{s}$ after the characteristic signal is observed. This is the time for the acoustic wave to feedback onto the surface of the transducer and affects the electrical signal at the transducer. The electrical signal at the transducer is shown in Figure 21. The characteristic signals associated with the homogeneous nucleation appear at $40 \mu\text{sec}$ to 0.1 msec depending upon the voltage amplitude of the ultrasonic signal. Comparing the characteristic signals for the similar pulse width (see Figure 18 and 20), one can see that they are more defined. The characteristic signal appears in the time range from $40\text{--}60 \mu\text{sec}$. The reason for this difference is unknown but we do know that the 1 MHz hemispherical transducer is bigger and heavier than the 2 MHz transducer with small aperture angle. The response time, i.e. the time for the acoustic energy to build up, is longer. We should also mention here that the intensity fluctuation for the 1 MHz hemispherical transducer seems to be greater than that for the 1 MHz transducer. The disturbance to the transmitted light

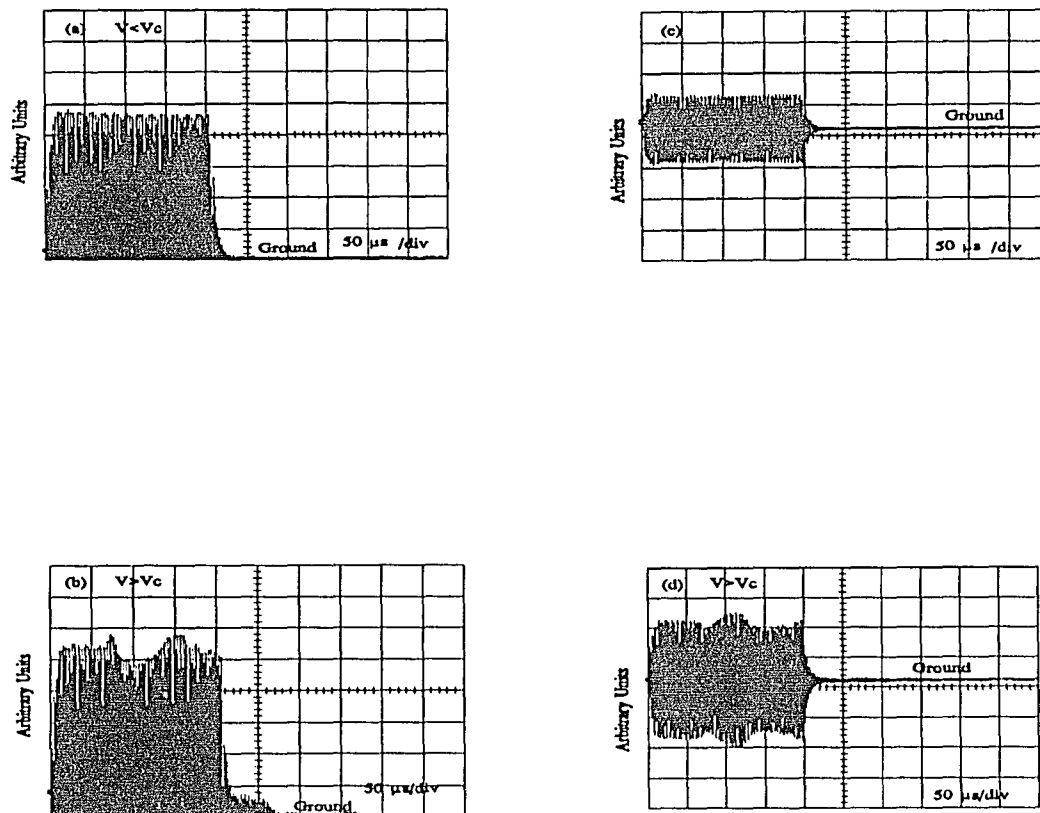


Figure 21. The electrical signals at the hemispherical transducer of 1 MHz. (a) and (c) are signals before the critical voltage V_c is reached. (b), and (d) are signals when the critical voltage is reached.

might depend on how strongly the ultrasonic wave is focused.

Following Debye's theory described in Chapter III, i.e. Equation (3.14) and utilizing the surface pressure amplitude, P_0 , which is determined using the method described in the Appendix, we performed the calculation of the tensile strength of liquid nitrogen for different bath temperatures. The measured bath temperature as a function of the tensile strength in the liquid at the focus is as shown in Figure 22. We have carried out the measurements of the tensile strength of liquid nitrogen using transducers with resonance frequencies of 1 MHz and 2 MHz in the temperature range from 77 K to near 100 K. In Figure 22, the data are obtained from four separate experiments. When the temperature in the liquid is below 90 K, the liquid is relatively more stable and consequently the measurement is easier to carry out. Above 90 K the higher vapor pressure causes more disturbance to the liquid nitrogen in the dewar. It is more difficult to obtain consistent results. We will discuss the heat leak of the dewar and instability of the liquid nitrogen later.

Possible uncertainties in the measurements come from the process of determination of the surface pressure at the transducer, the local heating which affects the temperature measurement, and the uncertainty of the critical voltage on the transducer. First, we estimated the uncertainty of the value of critical voltage to be less than 7% through varying

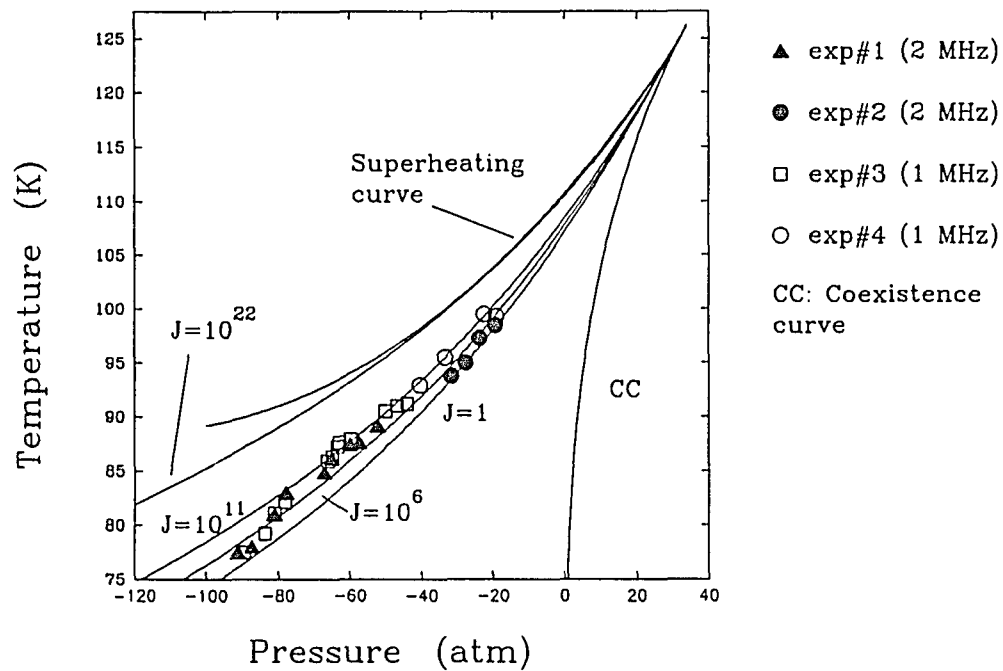


Figure 22. The experimentally obtained data in comparison with the theory of homogeneous nucleation for different transducers of 1 MHz and 2 MHz respectively.

the voltage and observing the transmitted light signal. Secondly, when shock waves are present in the liquid nitrogen, additional heating due to the absorption of acoustic energy must be considered. Nissen (1988) analyzed this local heating effect and obtained a temperature correction of about 25 mK in liquid helium. This temperature correction could be ignored if the temperature was above 2.6 K since the uncertainty brought by the measurement of surface pressure at the transducer was much larger. We will discuss the uncertainty of surface pressure amplitude in the Appendix A and the temperature corrections in Appendix B. The experimental results demonstrated in Figure 21 are the main results of this dissertation. Our experimental results have shown that most of the data points fall into the region from $J=10^6$ to $J=10^{11}$ bubbles/cm³ sec and they are in good agreement with the prediction from the classical nucleation theory. It seems that not only is the formalism of classical nucleation theory valid in the positive pressure region, which was shown by Sinha (1987), but also its validity can be extended to the negative pressure region. This is only the second cryogenic liquid next to liquid helium to reach the tensile strength predicted by the classical nucleation theory. The results in Figure 22 have several implications. Because we have used the same method as Nissen's, it is evident that this ultrasonic cavitation method can be used to measure the tensile strength of other liquids. To measure the tensile strength of a liquid

using the acoustic cavitation method, one has to use very short and intense focused ultrasonic pulses to avoid the possible interference by heterogeneous nucleation. The use of very long duration ultrasonic pulses causes lower apparent tensile strength. As the tensile strength is an intrinsic property of a liquid; it should not depend on the measurement method. The measured tensile strengths obtained from 1 MHz and 2 MHz transducers showed no obvious difference within the experimental range. Although we tried to be as rigorous as possible, this ultrasonic cavitation method is still a crude method to measure the tensile strength. We have neglected absorption, and also nonlinearity effects because of the lack of information on the content of higher harmonics.

MEASUREMENT OF THE TENSILE STRENGTH OF LIQUID NITROGEN USING RAMAN-NATH LIGHT DIFFRACTION METHOD

In order to further study the tensile strength of liquid nitrogen, we have tried to use the light diffraction method to measure the tensile strength independently. In this approach, one has to measure the transmitted light intensity for given voltage. However, we have met with an insurmountable difficulty with the apparatus that we have due to the heat leak problem. The temperature gradient from the inner wall to the top and then onto the outer wall causes a heat leak into the liquid nitrogen. One can observe the convection current from the windows. The consequence of this heat leak is that

the convection current disturbs the system and makes the transmitted light move around randomly. Even though it does not make a difference for detecting the moment when the homogeneous nucleation occurs since what we care about is to see the fluctuations of the transmitted light intensity, it does make our quantitative measurement of the intensity of transmitted light impossible. We have tried different ways to remedy the problem such as adding several insulation layers in the dewar to reduce the heat leak, but there is no significant improvement. The unstable characteristics of the transmitted light is as shown in Figure 23. One can see that the magnitude of transmitted light intensity varies so rapidly that it is impossible to get reliable results. Figure 23 shows that there are a lot of frequency components in the transmitted light intensity. To make sure it is not the result of any kind of noise due to the nearby electrical circuits or the interference of some kind of vibration of the system, the Fast Fourier Transform (FFT) is performed in order to obtain the frequency spectrum. Figure 24(a) shows the real time signal filtered by a 300 Hz lowpass filter for a sampling frequency of 10 kHz and 20000 points. Figure 24(b) shows its FFT results. Figure 25(a) shows the optical signal for sampling frequency of 200 kHz and 20000 data points, and Figure 25(b) shows its FFT results. The variations of real time optical signals for both Figure 24(a), 25(a) are very large. Considering the time period to perform the measurement

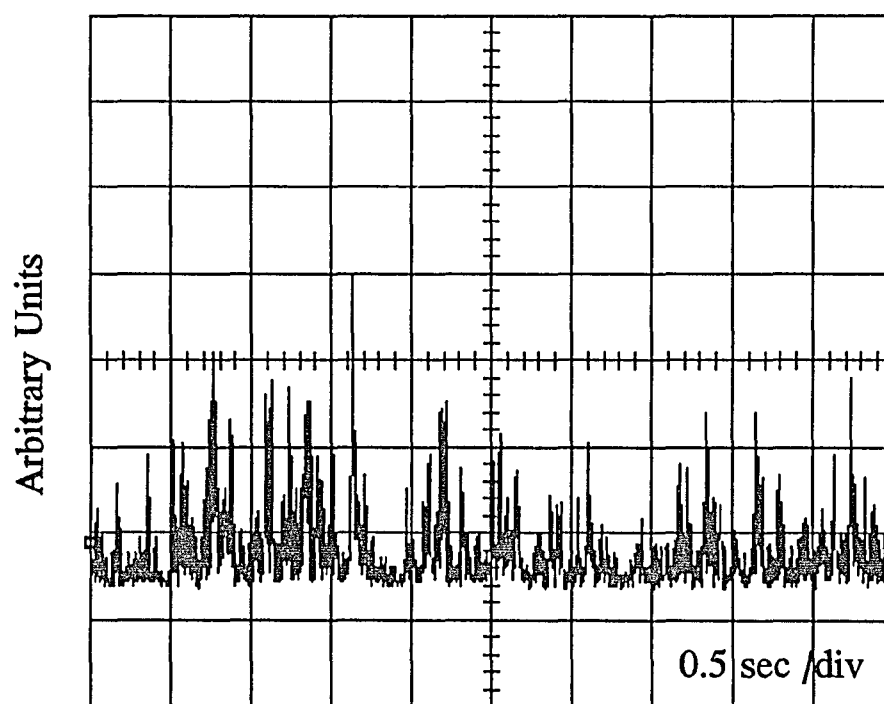


Figure 23. The intensity of transmitted light without the presence of the ultrasonic field.

of the tensile strength, which is less than a few tenths of microseconds, such a noisy background makes it impossible to carry out the measurement. The continuous characteristics of the FFT spectrum also suggest the above conclusion. On the other hand, even if one could possibly stabilize the liquid nitrogen in the dewar, it is still very difficult to determine the pressure accurately for large magnitude. From Figure 7, one can see that when the pressure amplitude is large, there are many different values of the Raman-Nath parameter that correspond to the same light intensity.

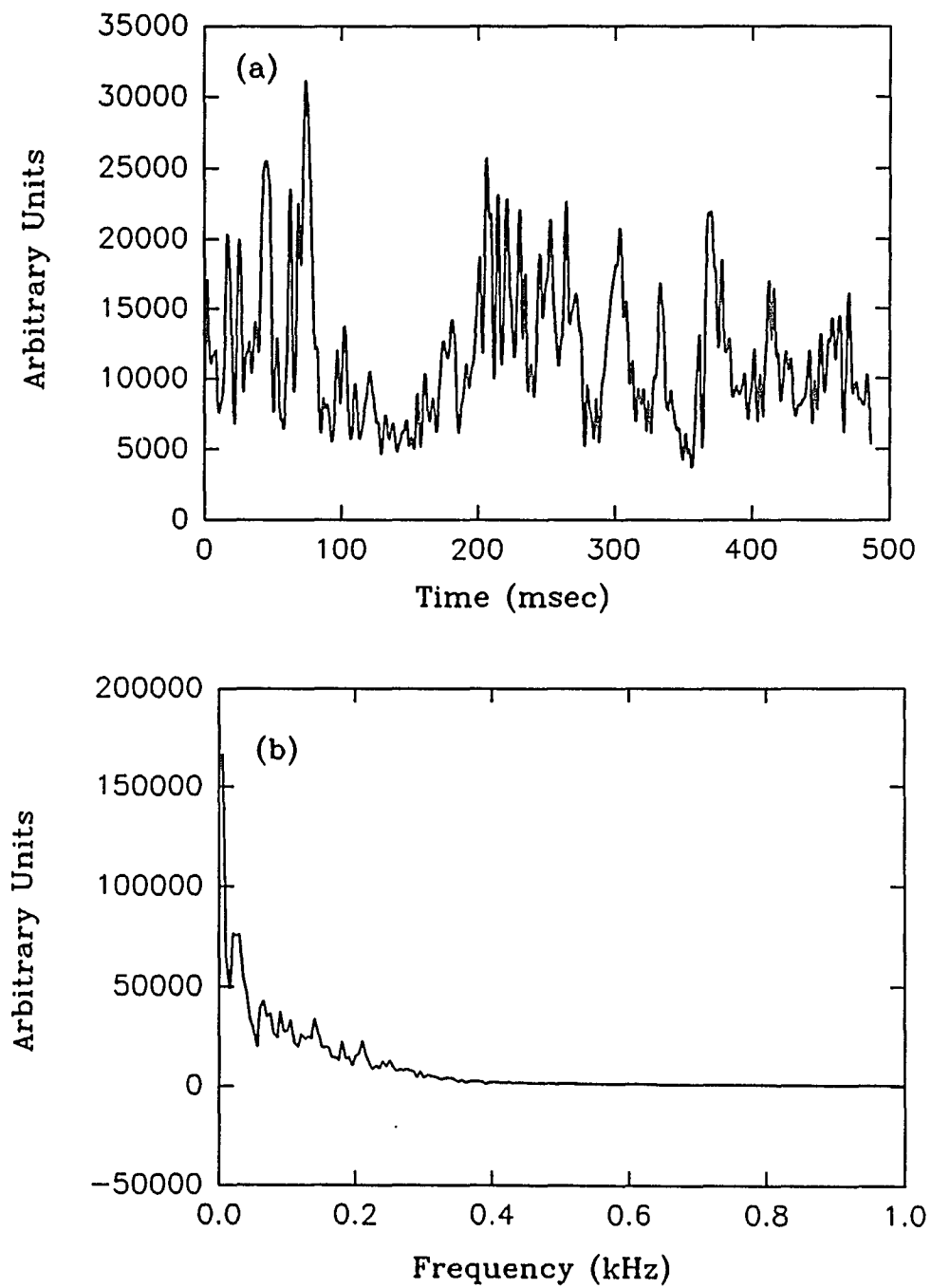


Figure 24. Optical signal in real time and frequency domain for sampling frequency of 10 kHz.

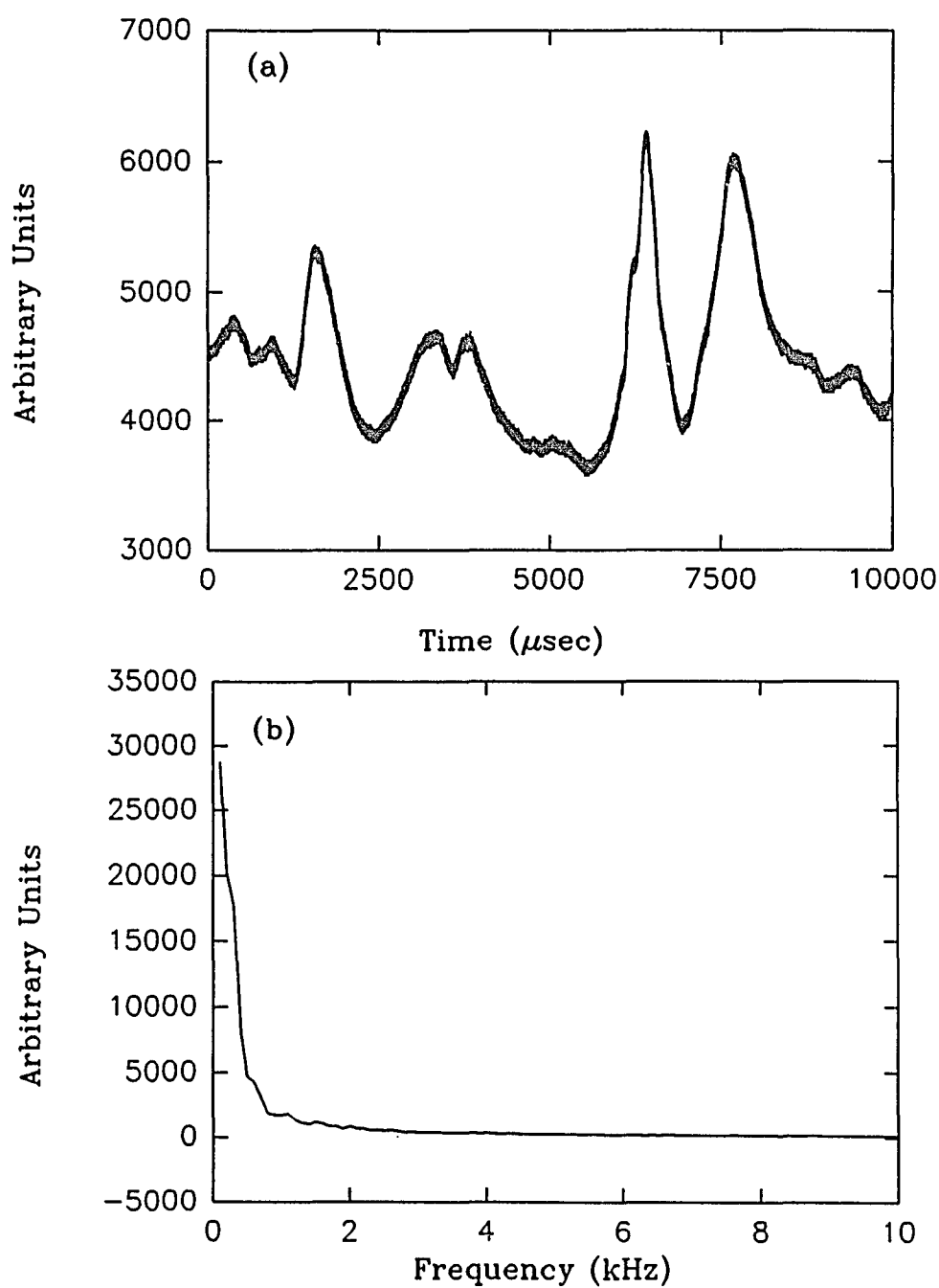


Figure 25. Optical signal in real time and frequency domain for sampling frequency of 200 kHz.

CHAPTER V

CONCLUSION

Although homogeneous nucleation of liquids has been studied extensively, it still remains as a puzzling subject. On the one hand, the classical nucleation theory developed by Becker, Doring and later authors has proven to be a good model for describing some liquid systems and it has met with great success in predicting the nucleation rates of the superheated liquids. On the other hand, except for a few cases, most of the reported experimental values of the tensile strength of liquids are far below the predictions of the classical nucleation theory. This work has provided the experimental evidence that for liquid nitrogen it is possible to reach the tensile strength as predicted by the classical nucleation theory. Besides liquid helium, this is only one other cryogenic liquid where the classical nucleation theory has been validated in the negative pressure region. Not only has this work enhanced our understanding of the homogeneous nucleation process and the tensile strength of liquids but also some aspects of light-ultrasonic wave interactions have been explored.

A careful analysis of various approaches to the study of homogeneous nucleation shows that a necessary condition to

obtain the true value of the tensile strength of a liquid is that any possible interference of heterogeneous nucleation has to be excluded and the liquid should be brought deep into the metastable region rapidly to avoid local heating. This requirement can be satisfied by focusing high intensity, pulsed ultrasonic wave into a small volume of the liquid. In contrast to liquid helium, the tensile strength of liquid nitrogen is so much higher that a shorter and more intense ultrasonic pulse is needed.

Different techniques for the determination of the acoustic amplitude at the focus of a concave spherical transducer have been studied extensively. Three methods investigated are light diffraction, Debye's theory and the KZK equation. The results from the experiments carried out in water have showed that those methods are valid in the pressure range studied and that they can be applied to the study of the tensile strength of liquid nitrogen. It is shown that the Raman-Nath theory, as modified by the introduction of an effective interaction length, can be used to determine the pressure amplitude in the focal plane of a focusing transducer with aperture angles of about 30° and the results obtained from different diffraction orders are consistent. Therefore in the focal plane the wavefronts can be approximated by plane waves and consequently the usual analysis can be made. Considering the nonlinearity, it was shown that as long as the nonlinearity is not too large, the experimental results follow

closely the calculated results. Moreover, it is shown that the light diffraction methods provides enough information to calculate the second harmonic content. In principle, it is possible that the content of the higher than the second harmonic can be obtained.

The measurement of the tensile strength of liquid nitrogen has been carried out and results have shown that the measured tensile strength is in good agreement with the prediction of the classical nucleation theory for nucleation rates between 10^6 to 10^{11} (bubbles/sec cm^3) in the temperature range tested. Only Debye's theory has been employed to obtain the tensile strength of liquid nitrogen and the absorption and nonlinearity of the liquid are ignored. The results obtained for the transducers with different resonant frequency have shown no difference within the range of experimental error. We also found that there is indeed a characteristic signal associated with the homogeneous nucleation onset which is similar to that is obtained from liquid helium.

This study of the tensile strength of liquid nitrogen is based on the fact that the classical nucleation theory has been confirmed for a long time in the positive pressure range and now it has been shown for the second and third time that it can be extended to negative pressure region.

REFERENCES

- Abeelee, K.V., Leroy, O. (1990) "Light diffraction by ultrasonic pulses: analytical and numerical solutions of the extended Raman-Nath equations," J. Acoust. Soc. Am. 88, 2298-2315.
- Achulichev, V.A. (1986) "Acoustic cavitation in low-temperature liquids," Ultrasonics 26, 8-18.
- Apfel, R.E. (1972) "The tensile strength of liquids," Scientific American 227, 6, 58-71.
- Apfel, R.E. (1981) "Acoustic cavitation," Methods of Experimental Physics 19, 335-342.
- Baidakov, V.G., Khvostov, K.V., and Muratov, G.N. (1982a) "Surface tension of nitrogen, oxygen, and methane over a wide range of temperatures," Rus. J. Phys. Chem. 56 497-499.
- Baidakov, V.G. and Skripov, V.P. (1982b) "Superheating and surface tension of vapor nuclei in nitrogen, oxygen, and methane," Rus. J. Phys. Chem. 56, 499-501.
- Barker, J.A. and Henderson, D. (1967) J. Chem. Phys. 47, 3959.
- Beams, J.W. (1956) "Tensile strength of liquid helium II," Phys. Rev. 104, 880-882.
- Beams, J.W., (1959) "Tensile strength s of liquid argon, helium, nitrogen, and oxygen," Phys. of Fluids 2, 1-3
- Becker, R. and Doring, W. (1935) Ann. Phys. 24, 719.
- Bezverkhii, P.P., Martynets, V.G., Martynets, E.V., and Kukarin, V.F. (1986) "Metastable region in the scaling theory of critical phenomena," Sov. Phys. JETP 63 (3), 552-554.
- Biquard, P. and Lucas, C.R. (1932) Acad Sci. Paris, 195, 121.
- Blander, M. and Katz, J.L. (1975) "Bubble nucleation in liquids," AIChE J. 21, 833-848.

- Briggs, L.J. (1950) J. Appl. Phys. 21, 721-722.
- Carlson, G.A., Henry, K.W. (1973) "Technique for studying dynamic tensile failure in liquids: application to glycerol," J. Appl. Phys. 44, 2201-2206.
- Cook, B.D. (1960) "Determination of finite amplitude distortion by light diffraction," J. Acoust. Soc. Am. 32, 336-337.
- Cook, B.D. (1965) "Optical method for ultrasonic waveform analysis using a recursion relation," J. Acoust. Soc. Am. 37, 172-173.
- Croxton, C.A. (1975) Introduction to Liquid State Physics, John Wiley & Sons, New York.
- Debye, P., (1909) Ann. Phys. New York, 30, 755.
- Dillmann, A. and Meier G.E.E (1990) "A refined droplet approach to the problem of homogeneous nucleation from the vapor phase," J. Chem. Phys. 94 (5), 3872-3884.
- Finch, R.D., Kagiwada, R., Barmatz, M. and Rudnick, I. (1964) "Cavitation in liquid helium," Phys. Rev. A 134, 1425-1428.
- Finch, R.D., Wang, T.G., Kagiwada, R., Barmatz, M. and Rudnick, I. (1966) "Studies of the threshold-of-cavitation noise in liquid helium," J. Acoust. Soc. Am. 40, 211-218.
- Frenkel, J., (1955) Kinetic Theory of Liquids, Dover, New York.
- Girshick, S.L. (1991) "Comment on: 'Self-consistency approach to the problem of homogeneous nucleation from the vapor phase,'" J. Chem Phys. 94 (1), 826-827.
- Green, J.L., Durben, D.J., Wolf, G.H., Angell, C.A. (1990) "Water and solutions at negative pressure: Raman spectroscopic study to -80 megapascals," (1990) Science, 249, 649-652.
- Hargrove, L.E. and Hiedemann, E.A. (1961) "Diffraction of wide and narrow light beams by distorted finite-amplitude progressive ultrasonic waves in water," J. Acoust. Soc. Am. 33, 1747-1749.

- Hargrove, L.E. (1968) "Effects of ultrasonic waves on Gaussian light beams with diameter comparable to ultrasonic wavelength," J. Acoust. Soc. Am. 43, 4, 847-851.
- Hargrove, L.E. (1968) Fourier series for intensity of a small gaussian light beam modulated by a progressive ultrasonic wave," J. Acoust. Soc. Am. 43, 6, 1448-1449.
- Hiedemann, E.A., Zankel, K.L. (1961) "The study of ultrasonic waveform by optical methods," Acustica 11, 213- 223.
- Hart, T.S. (1987) "Numerical investigation of nonlinear effects in focused sound beams," M.S. thesis, The University of Texas at Austin.
- Hart, S.T. and Hamilton, M.F. (1988) "Nonlinear effects in focused sound beams," J. Acoust. Soc. Am. 84 (4), 1488-1496.
- Jacobsen, R.T., Stewart, R.B., and Jahangiri, M. (1986) "Thermodynamic properties of nitrogen from the freezing line to 2000 K at pressures to 1000 MPa," J. Phys. Chem. Ref. Data 15, 735-797.
- Jarman, P.D., and Taylor, K.J. (1966) "Sonically induced cavitation of liquid helium," J. Low Temp. Phys. 2, 389-402.
- Kac, M., Uhlenbeck, G.E., and Hemmer, P.C., (1963) J. Math. Phys. 4, 216-228.
- Kashkooli, H.A., (1984) "Use of ultrasonic waveform distortion to measure the acoustic parameter of nonlinearity in water, methanol, liquid nitrogen, and helium," Ph.D. Thesis, University of Maine at Orono.
- Kashkooli, H.A., Dolan, P. J., and Smith, C. W. (1987) "Measurement of the acoustic nonlinearity parameter in water, methanol, liquid nitrogen, and liquid helium-II by two different methods: a comparison," J. Acoust. Soc. Am. 82, 2086 (1987).
- Katz, J.L., Blander, M. (1973) "Condensation and boiling: corrections to homogeneous nucleation theory for nonideal gases," J. Colloid Interf. Sci., 42, 496-502.
- Khokhlov, E.A., and Zabolotskaya, R.V., (1969) "Quasi-plane waves in the nonlinear acoustic of confined beams," Sov. Phys. Acoust. 16, 35-40.

- Klein, W.R., Cook, B.D., and Mayer, W.G. (1965) "Light diffraction by ultrasonic gratings," Acustica, 15, 67-74.
- Klein, W.R., and Cook, B.D. (1967) "Unified approach to ultrasonic light diffraction," IEEE Trans. Sonics and Ultrasonics, (SU) 14, 123-134.
- Kuznetsov, V.P., (1971) "Equations of nonlinear acoustics," Sov. Phys. -Acoust. 16, 467-470.
- Kwiek, P. (1989) "Light diffraction by two spatially separated ultrasonic waves," J. Acoust. Soc. Am. 86, 2261-2272.
- Levin, V.M., Lobkins, O.T., and Maev, R.G. (1987) "Field of a spherical focusing transducer with arbitrary aperture angle," Sov. Phys. Acoust. 33, 87-89.
- Leroy O., and Claeys, (1984) "Diffraction of light by profiled ultrasound," Acoustica 55, 21-25.
- Lothe, J. and Pound, G. M., J. Chem. Phys., 36, 2080 (1962).
- Maris, H.J. (1991) "Critical phenomena in ^3He and ^4He at $T=0$ K," Phys. Rev. Lett. 55, 45-47.
- Maris, H.J., Xiong, Q. (1989) "Nucleation of bubbles in liquid helium at negative pressure," Phys. Rev. Lett. 63, 1078-1081.
- Misener, A.D., and Herbert, G.R., (1956) "Tensile strength of liquid helium II," Nature 177, 946-947.
- Nagai S., (1986) "Acoustic power measurements of focused waves: radiation force and Raman-Nath methods," J. Acoust. Soc. Jpn. (E) 7, 4, 229-231.
- Narsimhan, G. and Ruckenstein, E. (1989) "A new approach for prediction of the rate of nucleation in liquids," J. Colloid and Interf. Sci. 128 (2), 549-565.
- Nissen, J.A., Bodegom, E., Brodie, L.C., and Semura, J.S. (1988) "New measurements of the tensile strength of ^4He ," Advances in Cryog. Eng. 33, 999-1003.
- Nissen, J.A., (1988) "Tensile strength of liquid nitrogen," Ph.D. Thesis in ESR/Physics Ph.D. program, Portland State University.

- Nissen, J.A., Bodegom, E., Brodie, L., and Semura, J. (1989) "The tensile strength of liquid helium," Phys. Rev. (B) 40, 6617-6624.
- Neppiras, E.A., and Finch, R.D. (1972) "Acoustic cavitation in helium, nitrogen, and water at 10 kHz," J. Acoust. Soc. Am. 52, 335-343.
- Nowakowski, B. and Ruckenstein, E. (1990) "A kinetic approach to the theory of nucleation in gases," J. Chem. Phys. 94 (2), 1397-1402.
- O'Neil, H.T. (1949) "Theory of focusing radiators," J. Acoust. Soc. Am. 21, 516-526.
- Oxtoby, D.W., Evans, R. (1989) "Nonclassical nucleation theory for the gas-liquid transition," J. Chem. Phys. 89, 7521-7530.
- Raman C.V., and Nath, N.S. (1935) Proc. Indian Acad. Sci. A 2, 406.
- Reiss, H., Katz, J.L., and Cohen, E.R. (1968) J. Chem. Phys. 48, 5553.
- Reibold, R. (1976) "The measurement of ultrasonic power using an acousto-optic method," Acustica 36,
- Ruckenstein, E. and Nowakowski, B. (1990) "A kinetic theory of nucleation in liquids," J. Colloid and Interf. Sci. 137 (2), 583-592.
- Shi, G. and Seinfeld, J.H. (1990) "Homogeneous nucleation in spatially inhomogeneous systems," J. Appl. Phys. 68 (9), 4550-4555.
- Sinha, D.N., Semura, J.S. and Brodie, L.C. (1982) "Homogeneous nucleation in 4He: a corresponding-states analysis," Phys. Rev. (A), 26 (2), 1048-1061.
- Sinha, D.N., Brodie, L.C., and Semura, J.S. (1987) "Liquid-to-vapor homogeneous nucleation in liquid nitrogen," Phys. Rev. (B) 36, 4082-4085.
- Sliwinski, A. (1990) "Acousto-optics and its perspectives in research and applications," Ultrasonics 28, 195-213.
- Temperley, H.N.V. and Trevena, D.H. (1977) "Metastability of phase transitions and the tensile strength of liquids," Proc. Royal Soc. 8, 395-402.

- Trevena, D. H., Cavitation & Tension in Liquids, Adam Hilger, Bristol and Philadelphia, (1987).
- Tjotta, N.J. and Tjotta, S. (1981) "Nonlinear equations acoustics, with application to parametric acoustic arrays, " J. Acoust. Soc. Am. 69, 1644-1652.
- Volmer, M. and Webber, A. (1926) "Nucleus formation in supersaturated systems," Z. Phys. Chem. 119, 277.
- Wagner, W. (1973) "New vapor pressure measurements for argon and nitrogen and a new method for establishing rational vapor pressure equations," Cryogenics 8, 470-482
- Xiong, Q., H.J. Maris, "Study of cavitation in superfluid helium-4 at low temperatures," J. Low Temp. Phys., Nos 3/4, (1991).
- Xiong, Q., (1991) "The tensile strength of helium II," Ph.D. thesis, Brown University.
- Zankel, K.L., and Hiedemann, E.A. (1959) "Diffraction of light b ultrasonic waves progressing with finite but moderate amplitudes in liquids," J. Acoust. Soc. Am. 31, 44-54.
- Zelenka, J., (1986) Piezoelectric Resonators and their Applications Elsevier, New York, 1986.
- Zeldovich, (1943) see Frenkel, J. (1955) Kinetic Theory of Liquids Dover, New York.

APPENDIX A

CALCULATION OF THE SURFACE PRESSURE OF A TRANSDUCER

APPENDIX A

CALCULATION OF THE SURFACE PRESSURE OF A TRANSDUCER

To obtain the pressure at the focus, one needs to know the pressure on the surface of the acoustic transducer. This pressure can be calculated from the electrical properties of the transducer and the power supplied to it. As shown by Zelenka the electric properties of a piezoelectric transducer can be modeled by an equivalent electric circuit consisting of resistors, capacitors, and an inductor. Usually, this model deals with the flat plate transducer. We apply it to the focusing transducer based on the argument that the diameter of the transducer is much larger than the thickness. The circuit diagram is shown in Figure 26. The total electrical impedance of the transducer at a particular frequency is found to be

$$Z_T(\omega) = \frac{\omega L - \frac{1}{\omega C} - jR_T}{\omega C_0 R_T + j[\omega C_0 (\omega L - \frac{1}{\omega C}) - 1]} \quad (A1)$$

After measuring the impedance at different frequencies, the parameters of the model can be obtained by a least-square fit. When the transducer is submerged in the liquid, R_T equals R_A , the equivalent electrical resistance due to the acoustic load presented by the liquid to the transducer plus

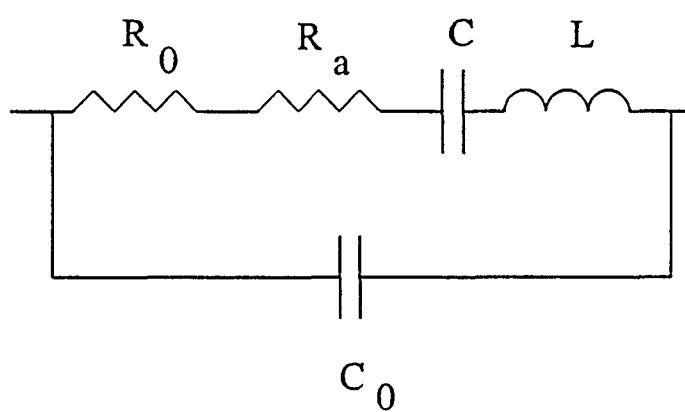


Figure 26. The equivalent circuit of a focusing transducer. $R_T = R_0 + R_A$.

R_0 , the resistance due to the supports. With the transducer suspended in air, R_T is equal to the same support resistance plus the radiation resistance of the air. But since this resistance is proportional to ρc , with ρ the density and c the speed of sound in the medium, it is negligible in air. Thus we essentially measure R_0 in the latter case. Since the acoustic energy radiated into the liquid is equal to the electrical energy, E , dissipated in R_A , one obtains the following:

$$E = \frac{V^2}{R_a} = \frac{P^2 A}{2 \rho_0 c} \quad (A2)$$

where P is the pressure amplitude at the surface of the transducer, ρ_0 is the density of the liquid, V is the calculated voltage driving R_A , and A is the surface area of the transducer.

We set up a gate circuit as shown in Figure 27. The ratio of output and input voltage can be expressed as

$$\frac{V_1}{V_2} = \frac{Z_1 + R_2}{R_2} \quad (A3)$$

where Z_1 is given by

$$\frac{1}{Z_1} = \frac{1 - \omega C_0 (\omega L - 1/\omega C) + j \omega C_0 R_0}{R_0 + j (\omega L - 1/\omega C)} \quad (A4)$$

By measuring the input and output voltage at the different

frequencies and using the least-square fitting method we obtain the values for the resistance, the capacitances, and the inductance. Therefore the surface pressure can be determined.

The resultant fitted curves are shown in Figures 28 and 29 which show the data in air and water respectively. The parameters of both the 1 MHz and 2 MHz transducers were measured using the same method as shown in Figure 30, 31. The repeated measurements of the parameters for the same transducer showed that a maximum uncertainty is about 15 percent because of the experimental errors and process of the least-square-fitting.

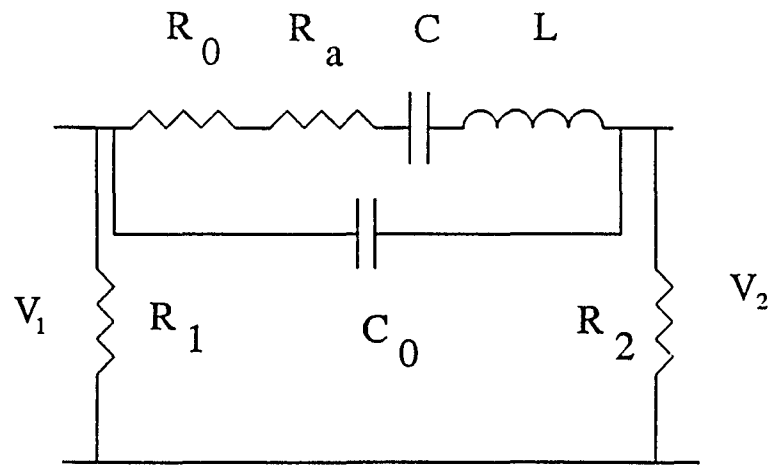


Figure 27. The gate circuit measuring the impedance of the transducer.

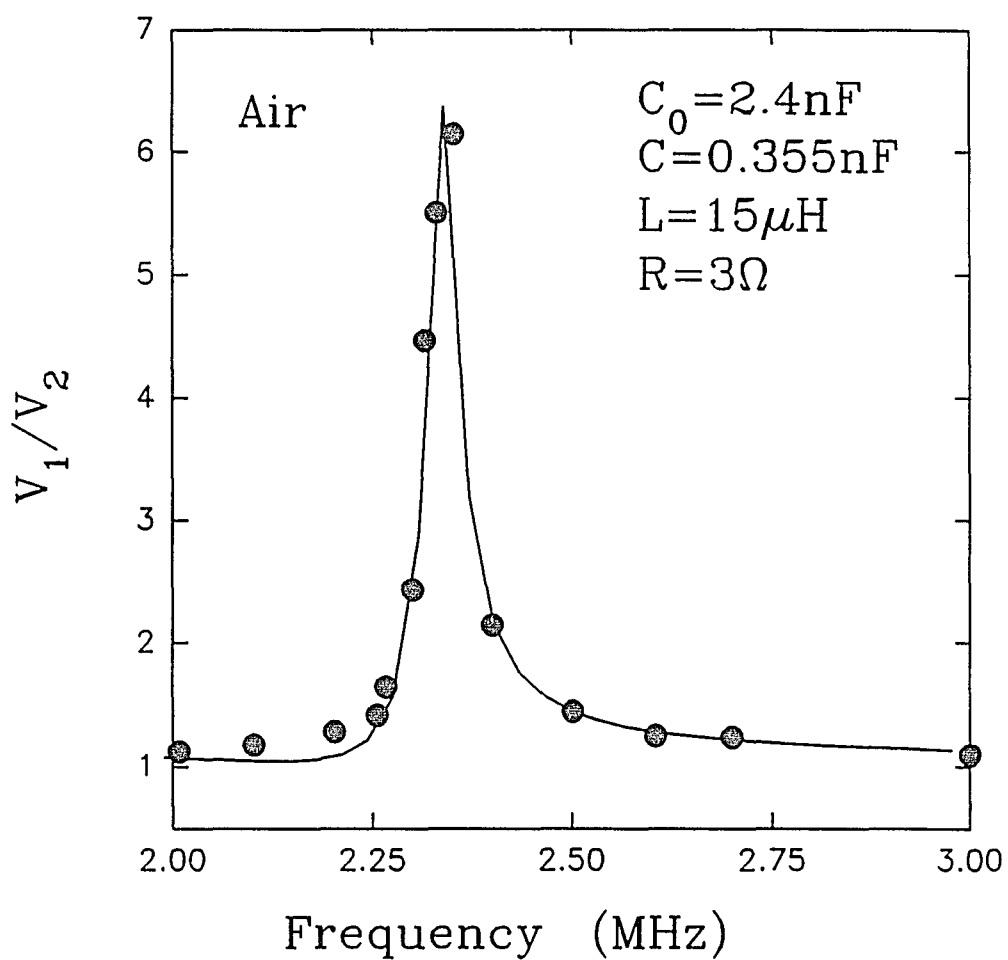


Figure 28. Measured ratio of V_{in}/V_{out} as a function of frequency when the transducer is in air at room temperature.

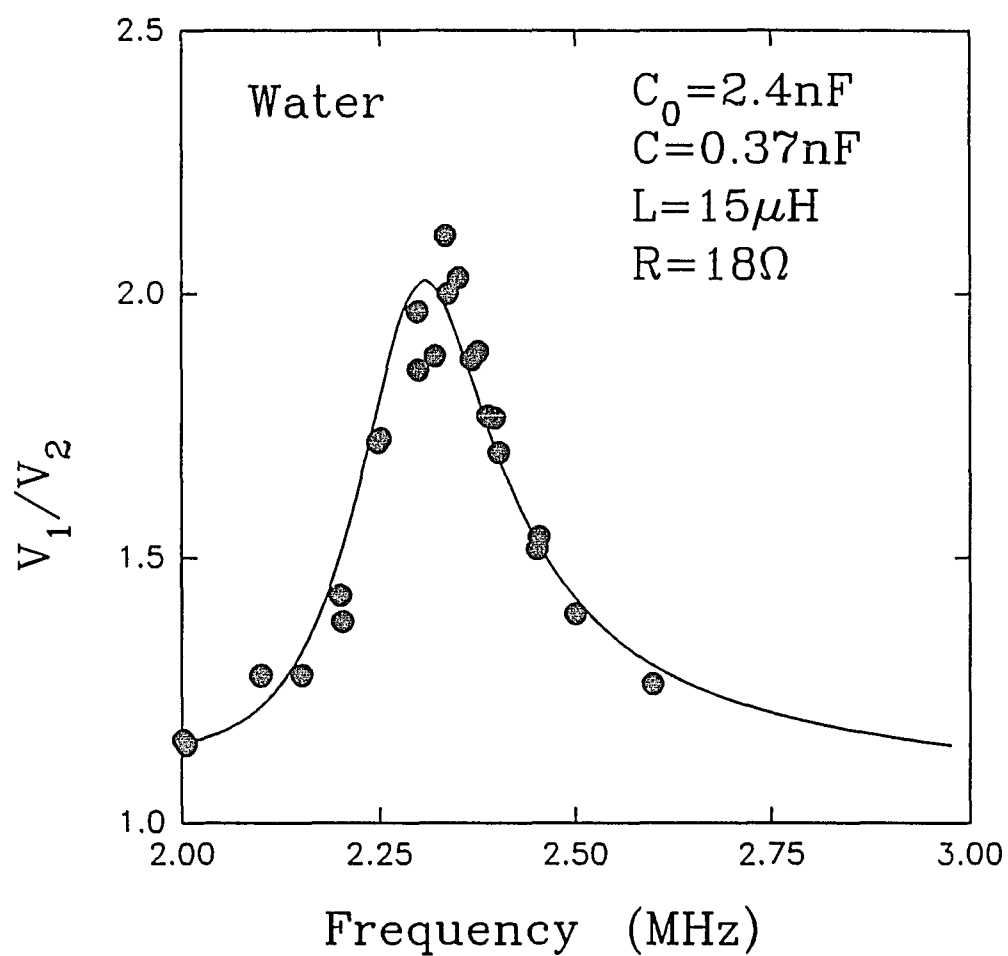


Figure 29. Measured ratio of V_{in}/V_{out} as a function of frequency for the transducer in water.

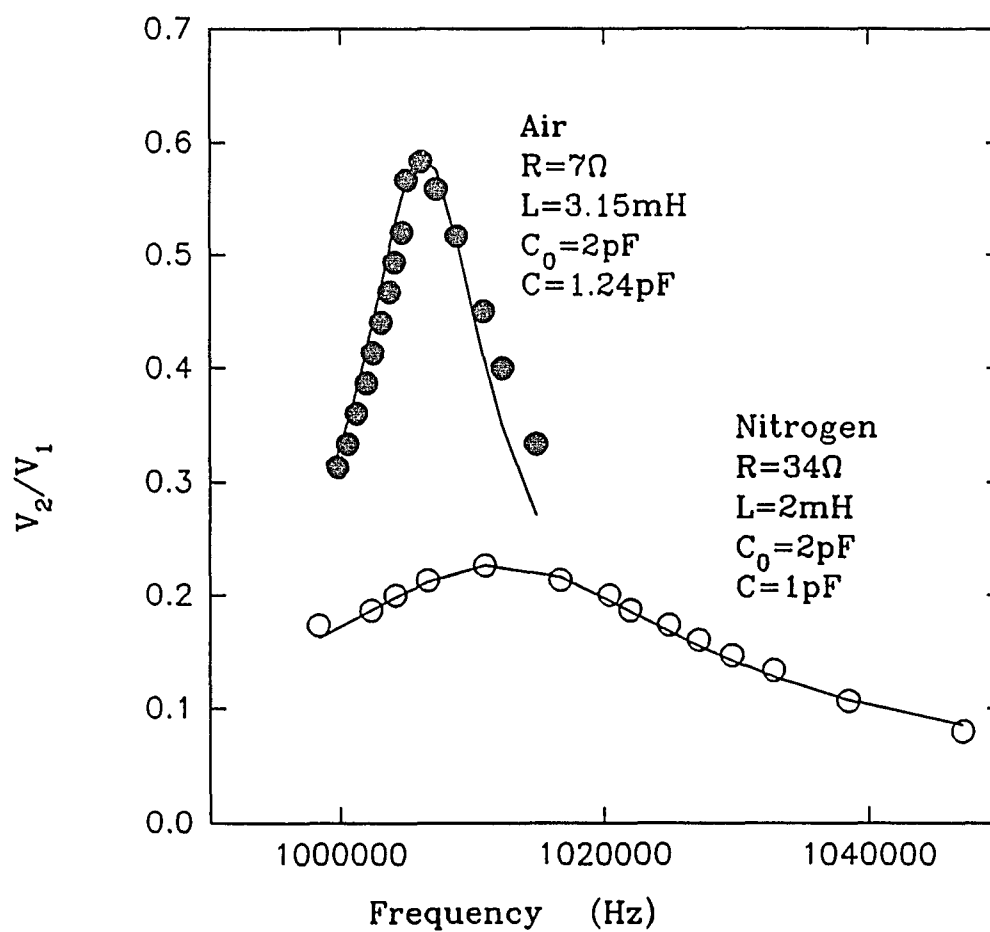


Figure 30. Measured ratios of $V_{\text{out}}/V_{\text{in}}$ as functions of frequency for the transducer of 1 MHz in air and liquid nitrogen.

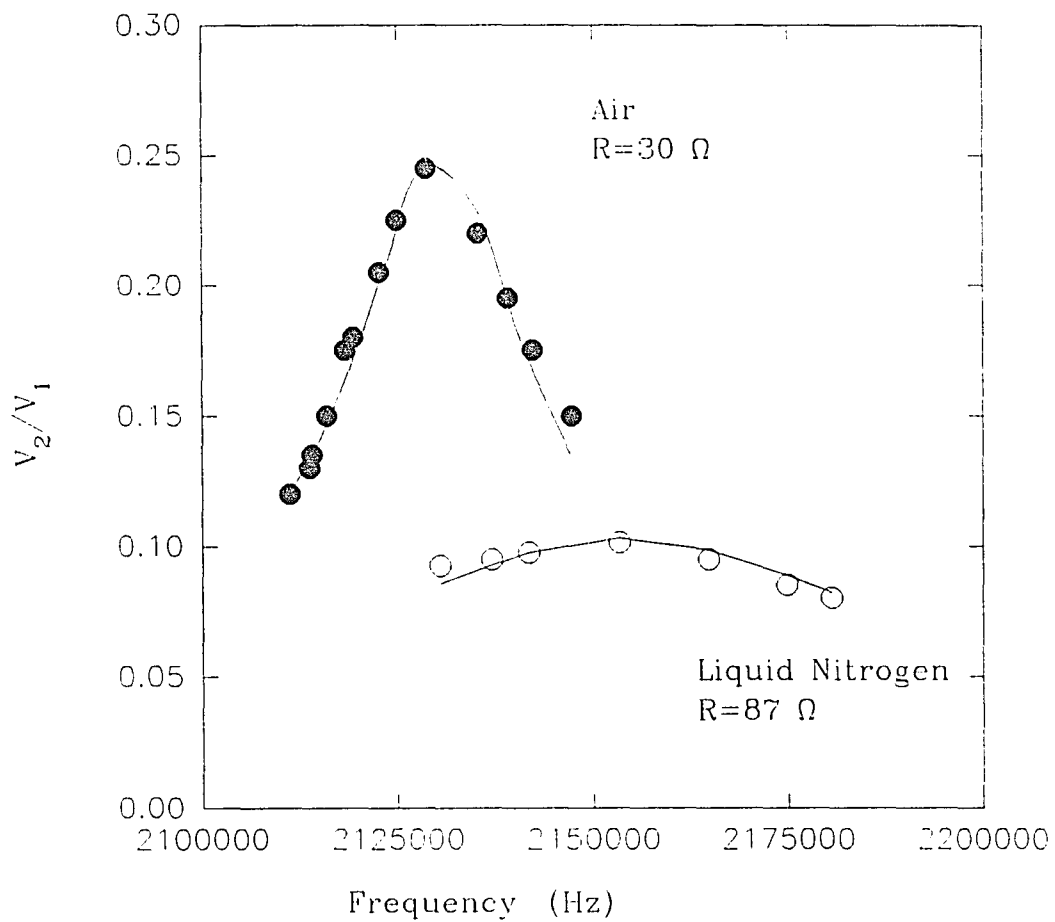


Figure 31. Measured ratios of V_{out}/V_{in} as functions of frequency for the transducer of 2 MHz in air and liquid nitrogen.

APPENDIX B

CORRECTION OF THE TEMPERATURE MEASUREMENT

APPENDIX B

CORRECTION OF THE TEMPERATURE MEASUREMENT

In Fig. 20, the temperature at the focal region is assumed to be equal to that of the bulk liquid. In fact, the local temperature changes with the variations of the local pressure amplitude. Therefore, the need for temperature corrections is investigated. This issue has been discussed for liquid helium by Nissen (1988). We will apply his method to liquid nitrogen.

If no shock wave is present, then the compression and rarefaction of the acoustic wave takes place adiabatically. The temperature change can be estimated from the thermodynamic relation

$$TdS = 0 = C_p dT - TV\alpha_p dP \quad (B1)$$

where C_p is the specific heat capacity at constant pressure and V is the specific volume and α_p is the volume expansivity at constant pressure. Equation (B1) can be integrated to find the temperature change if C_p and α_p are known as functions of P and T . Unfortunately, this is not the case. The best that can be done is to find the functional form of C_p and α_p in the stable liquid region and to extrapolate into the metastable region. However, the problem can be simplified one step further since the maximum

correction is small. For liquid nitrogen, the maximum correction applicable to the experiments is when the vapor pressure is about one atmosphere and the temperature is equal to 78 K. We have:

$$dP = -10^7 \text{ Pa}$$

and

$$C_p = 57.31 \text{ (J/mol K)}$$

Substituting,

$$\alpha_p T = 0.378 ,$$

$$V = 3.486 \times 10^{-5} \text{ m}^3/\text{mol} ,$$

and

$$T = 78 \text{ K}$$

into Eq. (B1) to obtain the temperature correction

$$\Delta T = 2.31 \text{ K} \tag{B2}$$

This is about three percent of the measured value of the temperature.

When shock waves are present in the liquid nitrogen, additional heating due to the absorption of acoustic energy may need to be considered. To estimate the magnitude of this heating, it is also sufficient to examine the effect of shock waves near 78 K, where the acoustic amplitude is the greatest and the value of the heat capacity is the smallest in the temperature range that we investigate. Following Nissen (1988), if it is assumed that the energy is absorbed uniformly by the mass of liquid nitrogen in the focal region, then the temperature rise ΔT , is given by

$$\Delta T = \frac{\Delta E}{m C_p} \quad (B3)$$

where ΔE is the acoustic energy lost from the fundamental. All of this energy is assumed to be dissipated as heat.

$$\Delta E = \frac{P_f^2 - P_f'^2}{2\rho c} A \Delta t \quad (B4)$$

where P_f is the pressure amplitude of the fundamental harmonic without higher order harmonics and P_f' is the pressure amplitude of the fundamental harmonic with the presence of higher order harmonics, ρ and c are the density and the speed of sound at 78 K, A is the area of focal region facing the acoustic beam, Δt is the time period for the shock wave to reach the focal region. By assuming that the focal region has a volume of 1 mm^3 and using $\rho c = 7.4 \cdot 10^5 \text{ (kg/m}^2\text{sec)}$, $C_p = 2.006 \cdot 10^3 \text{ (J/kgK)}$, and density of liquid nitrogen = 830 kg/m^3 , one can obtain

$$\Delta T = 0.41 K \quad (B5)$$

In this calculation we assume that the pressure amplitude of the higher harmonics is twenty percent of the fundamental. Even with the over estimation of the content of the higher harmonics, the temperature rise due to the absorption of the shock wave is about 0.5 K.